AD656719

COLUMBIA UNIVERSITY
IN THE CITY OF NEW YORK

LAMONT GEOLOGICAL OBSERVATORY
PALISADES, NEW YORK

MICROTOPOGRAPHY OF THE BLAKE-BAHAMA REGION

by

G. M. Bryan and R. G. Markl

Technical Report No. 8
CU-8-66-NObsr 85077

DECEMBER 1966

54

MICROTOPOGRAPHY OF THE BLAKE-BAHAMA REGION

by

G. M. Bryan and R. G. Markl

Technical Report No. 8

CU-8-66 Contract NObsr 85077

December 1966

INTRODUCTION

Over most of the North Atlantic the topography which influences bottom loss is relatively large scale - large enough laterally to be resolved for the most part by the main beam of the usual 12 kc echo sounder (beam width roughly 30°). As a result, echo sounder records have proved useful in predicting bottom loss over the North Atlantic, to a first approximation, on the basis of topography. In the vicinity of the Blake-Bahama Basin and Outer Ridge, however, it has been found that relatively small-scale topography plays an important role in bottom loss. There are extensive areas of rolling topography with periodic features that are just resolvable in the main beam. Beyond this resolvable range records show closely-spaced, overlapping, hyperbolic echoes extending for many miles over topography which is relatively smooth on a larger scale. In many of these records the individual hyperbolic traces are not sharply delineated but have a characteristically fuzzy or blurred appearance. Occasionally this fuzziness persists into areas where no hyperbolas are discernible and the trace, although fuzzy, looks quite flat. Measurements in the area indicate that bottom loss is significantly greater over these types of bottom. In areas where the large scale topography appears quite smooth but the echo sounder trace is fuzzy, bottom loss can be high.

Therefore a detailed study of the micro-topography of the Blake-Bahama Region was undertaken. The principal aim was to define the extent of the zones of fuzzy bottom as shown on 12 kc echo sounder records and to include this characteristic as a parameter in the prediction of bottom loss on the basis of echo sounder records. Preliminary results were reported by Bryan (1964) and Bryan and Ewing (1964).

As suggested above, it is convenient to classify the PDR data into four categories: regional topography, periodic topography, hyperbolic echoes, and incoherent or "fuzzy" traces.

REGIONAL TOPOGRAPHY

The regional topography of the Blake-Bahama area has been discussed by Pratt and Heezen (1964). Bathymetric contours shown in Fig. 1 are based on all available LGO tracks through November 1966 in addition to a large number of tracks run by USS COMPASS ISLAND in 1958. Following the usual terminology we distinguish from west to east, the Blake Plateau, the steep Blake Escarpment, the Blake-Bahama Basin, the Blake Outer Ridge, and the Hatteras Abyssal Plain. The sounding lines involved are shown superimposed on the bathymetry in Fig. 2 (foldout).

Details within the ridge zone include the crest of the main ridge which branches off from the Escarpment at about 32°30'N, running roughly southeast, and a secondary ridge which branches off at the "nose" of the Escarpment at about 30°N, parallels the main crest to about 28°N and then curves westward, forming the eastern boundary of the Blake-Bahama Basin. North of the ridge zone at about 34°N-73°W the mouth of the Hatteras Canyon opens into the Hatteras Abyssal Plain.

PERIODIC TOPOGRAPHY

Approximately periodic, smoothly undulating topography near the limit of resolution of the sounder beam has been labeled "periodic" in Fig. 2. In a few striking cases (Fig. 3 for example) the trace is quite periodic and appears almost sinusoidal; however, the category includes all approximately periodic topography in the size range and with relatively smooth curvature. Apparent wavelengths run roughly from one to six nautical miles, amplitudes from ten to forty fathoms.

In several instances different apparent wavelengths obtained from tracks run on different courses at the same location made it possible to establish the fact that these are linear features and to estimate their true wavelength and direction. In general, two tracks specify two possible directions, each with an associated wavelength; a third track is required to remove the ambiguity. The results show that the axes of these corrugations tend to parallel the contour lines (Fig. 2) and have true wavelengths of about 1 to 3.8 miles. This type of topography predominates on the lower continental rise along the northern border of the Hatteras Abyssal Plain, where the linear trends are quite marked, and along the flanks of the southern end of the ridge. Directly south of the tip no linear trends are apparent. The almost sinusoidal corrugations of Fig. 3 occur on the western slope of the smaller ridge (see location map, Fig. 7).

HYPERBOLIC ECHOES

The most prevalent type of abnormal trace in the area is made up of closely-spaced, overlapping hyperbolic echoes (Fig. 4b & 4d). For the most part, there is a fairly high degree of uniformity in the spacing and shape of the echoes and they tend to be roughly tangent to an apparent sea floor which is relatively smooth. This suggests small regularly-spaced linear features which are being crossed at an angle by the sounding track. The lateral dimensions of the features, in a direction perpendicular to their linear trends are too small to be resolved by the echo sounder beam. Trend directions in this type of topography can be estimated from a knowledge of the shape of the hyperbolic trace and the speed of the ship. Specifically, for a point topographic feature the shape of the trace depends on the speed of the ship over the feature. The problem of computing the ship's speed in terms of echo shape from point topographic highlights is discussed by Luskin, Nafe, and Ewing (1957). If the feature is a line rather than a point, and the ship crosses the line at a speed v and an angle Θ (Fig. 5a), then the echo trace will be sensitive only to the velocity component $v_a = v\sin\Theta$ perpendicular to the feature. Thus comparison of true ship's speed with apparent speed computed from the echo trace yields the inclination Θ of the line from the ship's track. The result does not distinguish between clockwise and counterclockwise senses of the inclination and a second track is required to remove the ambiguity.

Computation of the apparent speed v_a was based on an approximation which makes use of the fact that ship's speed (~ 5 meters/second in this case) is small compared with sound speed (1500 m/s). The trace then approaches an exact hyperbola given by (see Fig. 5b):

$$\left(\tfrac{1}{2}\, VT\right)^2 - (v_a\, t)^2 = \left(\tfrac{1}{2}\, VT_m\right)^2$$

where T is the two-way travel time of the pulse, measured when the ship s is a time t away from the point of closest approach P to the feature at Q. V and v_a are sound speed and apparent ship's speed respectively. Although we could solve this equation for v_a in terms of V, t, T, and T_m, as was done by Luskin, et al, it is often difficult to measure t as accurately as the other quantities. Alternatively, therefore, we differentiate the above equation and eliminate t. The result,

$$v_a = \tfrac{1}{2}V \frac{T}{\sqrt{T^2 - T_m^2}} \quad \frac{dT}{dt} ,$$

gives the apparent velocity in terms of V, T, T_m and the slope dT/dt of the trace at T. This method gave consistent results and was found especially useful where only half the hyperbola was visible. Trend lines were computed in this way in several instances where tracks showing hyperbolas intersected. Once again the trends are consistently parallel to the bathymetric contours. Hyperbolic echoes are found chiefly on both flanks of the main ridge and on the western flank of the secondary ridge, where they extend well into the Blake-Bahama Basin (see also, Clay & Rona (1964)).

FUZZY TRACES

An example of the characteristic fuzziness often encountered in the echograms of the area is shown in Fig. 4c. This should be compared with the normal trace shown in Fig. 4a. The normal echoes are strong and well-aligned, producing a sharp leading and trailing edge on a trace whose width faithfully reflects the length of the outgoing ping. In the fuzzy traces the echoes are faint and ping-to-ping alignment is poor. Although intermediate cases can be found, ranging between the two extremes shown, the traces in the area are more often either good or bad, and transition between good and bad is often remarkably abrupt as in Fig. 6 (see Fig. 7 for location).

In the older records, with longer ping lengths, these fuzzy traces were often associated with topography that appeared to be quite smooth and flat. More recently the ping length has been kept as short as possible and in nearly all cases of fuzziness in the later records hyperbolas are discernible to some extent. Fig. 6 shows traces taken with two different ping lengths in the same area. The increased resolution as the ping length is varied from about 18 ms in (a) to about 3 ms in (b) is quite evident. The fuzzy uneven texture persists to some extent, however. This dependence on ping length is largely responsible for the inconsistencies sometimes found in Fig. 2 at points where tracks of different cruises cross. Generally speaking, however, regions of concentrated fuzziness tend to coincide roughly with those where hyperbolas are present. On the basis of the tracks shown in Fig. 2 the area involving hyperbolic and fuzzy topography has been delineated in Fig. 8. North of the prominent nose feature of the Blake Escarpment ($\sim 30^{\circ}$N) this topography is rather sharply bounded on the west by the 1600 fathom contour. This boundary can be correlated with an unconformable change in sedimentary regimes observed on seismic profiler records. Hyperbolic and fuzzy topography is largely absent from the crest of the main ridge.

The dependence on ping length, the tendency for areas of fuzziness to coincide with areas of hyperbolas, and the lack of ping-to-ping alignment in the fuzzy trace suggest that the fuzzy trace results principally from small-scale topography of the water-sediment interface rather than from unusual acoustical properties of the sediment.

The usual plane-wave reflection coefficient for the water-sediment interface, which is appropriate for a plane wave reflected from a plane interface, depends only on these material properties and the angle of incidence. For a non-planar interface the shape of the interface must also be taken into account. For example, relatively gentle curvature will introduce a certain amount of focussing or defocussing (curvature of the reflected wavefront) but the reflection is still essentially specular. On the other hand a very rough interface will scatter the sound energy incoherently in all directions and no specular reflection will be possible. These two limiting cases are tentatively identified respectively with sharp and fuzzy PDR traces. The sediment material need not differ in the two cases, although sediment type no doubt is a condition of formation of the microtopography itself.

In the case of scattering from a rough surface the extent of scattering depends on the vertical and horizontal dimensions of the irregularities compared with the wavelength of the incident radiation. If the vertical dimensions are very small compared to the wavelength the scattering will be negligible regardless of the horizontal dimensions. If the vertical dimensions are of the order of a wavelength the scattering will be great for horizontal dimensions of the order of a wavelength but small for horizontal dimensions much larger than a wavelength. An opportunity to observe this dependence on wavelength is afforded to some extent by measurements made simultaneously with the 12 kc echo sounder and the seismic reflection profiler (about 100 cps). Results from simultaneous measurements are shown in Fig. 9. The records have been reproduced to approximately the same scale. They show a rather typical sudden transition from smooth flat bottom to fuzzy hyperbolas with peak-to-peak spacing of the order of 500 m. The seismic record (c) was made by a compressed air source at a repetition rate of about 15 seconds; the PDR records by a 12 kc transducer at a 1 second repetition rate. Records (b) and (c) were made simultaneously, just before the ship stopped for a station. During the station the ship drifted back approximately over its previous track. Record (a) is the PDR trace made as the ship left the station on the original course and before the profiler was back in operation. Records (b) and (c) can thus be compared feature for feature. However, since the PDR was inadvertently gated at the time, record (a) is included to permit overall comparison with an ungated trace.

In spite of the much slower repetition rate, the profiler produces sharper traces of individual features than does the PDR. Note especially the second hill from the left, which is quite evident in the profiler record but barely visible in the PDR. This suggests smaller scale topography superimposed on the features seen in the records. That such microtopography is present is shown by bottom photographs taken during the station. Small, sharply-crested ripples (Fig. 10) were apparent in 16 of the 20 frames comprising the station. In several frames parallel ripples are separated by about 2 meters as in the photographs shown. The features appear to be several centimeters high.

The effect of such topography in each case can be estimated very roughly by assuming equally-spaced parallel ridges 2 m apart with relief of perhaps 10-15 cm. Then for vertically incident radiation at 12 kc (wavelength $\lambda = 1/8$ m) the reflected radiation will be split up into various orders of diffraction with directions from the vertical given by the Bragg formula:

$$\sin\theta_n = \frac{n\lambda}{L} \approx \frac{n}{16}$$

where $L \approx 2$ m is the ridge separation. The specular reflection is given by $n = 0$ and is of course vertical. The first order diffraction peak ($n = 1$) is about $3\frac{1}{2}^{\circ}$ from vertical, and is therefore offset some 300 m from the transducer in a water depth of 5000 m. Thus only the specular term contributes. If the relief is approximated by a sinusoid with amplitude a, and the sediment is considered a fluid, the intensity of this term can be approximated, for $\lambda \ll L$, by (see for example, Officer, 1958)

$$I = I_o \left[J_o \left(4\pi \frac{a}{\lambda}\right) \right]^2$$

where I_o is the intensity returned from a plane surface (a=0) of the same impedance contrast, and J_o is the Bessel function of order zero. For $a \approx \lambda = 1/8$ m the envelope of $J_o\left(4\pi \frac{a}{\lambda}\right)$ is about .23 whence $I \approx 0.05\, I_o$. Thus the intensity returned to the transducer is only 5% of that expected for a plane surface.

For 100 cps $\lambda = 15$ m and all non-specular directions are imaginary since $\lambda > L$. In this case the non-specular or scattered portion is confined to the vicinity of the boundary and is lost to the specular term. In the long wavelength limit, $\lambda \gg L$, the sinusoidal model with amplitude = 12 cm and $L = 2$ m gives, to the same approximation, negligible loss due to the microtopography.

In summary, three types of abnormal or unusual PDR trace have been considered: periodic, hyperbolic, and fuzzy traces. In the area studied all three types are caused principally by bottom corrugations of different wavelengths. Hyperbolas generated by isolated point sources and rough, steep slopes such as the Blake Escarpment are not of interest here. The approximate range of wavelengths for each type is as follows:

periodic:	1000 - 7000 m
hyperbolic:	100 - 1000 m
fuzzy:	10 - 100 m

The sources of the majority of the periodic and hyperbolic echoes shown in Fig. 2 are of two types: (1) longitudinal ripples formed by bottom currents, as exhibited in the eastern Blake-Bahama Basin, (2) minor slumping and compressional folding such as is frequently seen on the eastern flank of the main ridge, for example.

The detailed study of topography in the 10-100 m wavelength range in deep water requires considerably more resolution than is possible with conventional surface-mounted echo-sounders and a much greater field of view than is afforded by bottom photography. One possibility is the use of a deep-towed echo-sounder, or at least a deep-towed pinger working into a ship-mounted receiver. Preliminary work with a deep-towed pinger in the area gave evidence of micro-relief but a detailed study was hampered by a large drift in the pinger time base. It is expected that future pinger lowerings will enhance our knowledge of the microtopography and its relation to bottom loss.

BOTTOM LOSS

As mentioned in the introduction, measurements in the Blake-Bahama area indicate that bottom loss is significantly greater over hyperbolic and fuzzy bottoms. A ship in this area, using a 4 kc system, found a 10-15 db increase in bottom loss while its 12 kc echo sounder (ping length $\sim$19 ms) simultaneously noted a gradual change from fairly coherent bottom trace to a very fuzzy or incoherent one (Weaver, 1957). This run of approximately 30 miles was made just east of the Outer Ridge (29°30'N; 72°40'W) at about three knots over what appeared to be practically smooth topography. The Lamont ship CONRAD was subsequently directed to duplicate the track with its 12 kc short ping sounder (ping length $\sim$5 ms). The CONRAD data, taken at 10 knots, disclosed microtopography indicated by hyperbolas and small periodic corrugations with wave-length and amplitude increasing in the direction of increasing fuzziness noted by the first ship. Calculation of the orientation of the corrugations at several points indicated that they are parallel to the regional contours. Subsequently the vertical exaggeration of the record made at 3 knots was increased by means of a flow camera, thereby accentuating details of topography which were not obvious in the original record. Fig. 11 shows (a) a portion of this modified record and (b) its equivalent CONRAD section.

OUTER RIDGE

In the process of investigating the echo sounder records in the area and plotting the extent of the fuzzy zones, it became apparent that these zones are related to the large scale structure of the Blake-Bahama Outer

Ridge, and therefore probably result from the processes forming the ridge.

The Blake Outer Ridge is an elongate feature over 300 miles in length which trends southeast from a point about 32°30'N, 76°30'W where it merges with the northern portion of the Blake Plateau. At this point the ridge is rather broad; it tapers down toward the southeast. The eastern flank is consistently steeper than the western.

The following discussion of the structure of the Outer Ridge is based upon detailed study of the character and behavior of the reflectors observed on continuous seismic reflection profiles along approximately 13,000 miles of ship's track. Three diagnostic sections are shown as Fig. 12 and oriented in Fig. 13. Both compressed air (sections AB & CD) and explosive (section EF) sound sources were used. Typical penetration in this area with these methods is 2 seconds of reflection time; the maximum penetration (3.5 sec) was achieved using explosives.

It is known that the Outer Ridge is a depositional feature (Ewing & Ewing, 1964) built upon Horizon A, an essentially flat-lying reflector of Cretaceous age which is present throughout the area of Fig. 2 east of the Blake Escarpment (see also, J. Ewing, et al, 1966). Above "A" we distinguish two major sequences divided by a reflector labelled x in Fig. 12. The lower lies directly on "A" and represents the major period of differential deposition which gives the ridge its relief; the upper has a more complex structure.

Post "A" sedimentation took the form of a mound of unevenly distributed acoustically transparent sediment. The poorly-defined reflector which tops this sequence, reflector x, can be traced throughout the Blake-Bahama Basin and secondary ridge provinces as well as over most of the

Outer Ridge. In section AB of Fig. 12 (which is a representative cross-section of this portion of the ridge) this layer thins abruptly toward the Hatteras Abyssal Plain from an estimated thickness of 1.5 sec at the ridge axis to only .5 sec in less than 50 miles; it thins more gradually toward the Blake Escarpment. The secondary ridge is displayed by this reflector, though its axis lies slightly to the east of the present topographic feature. In effect, the gross topography at the time reflector x was the sea floor was virtually the same as the present-day topography.

Post x sedimentation begins with .5 sec or more of acoustically transparent material which gradually gives way to series of thin parallel reflectors at about .5 sec below the bottom. Post x sedimentation is complicated north of 30°N in the ridge area by a reflector (y in Fig. 12) intermediate between reflector x and the sea floor. In the area of Fig. 2 this reflector is visible only under the crest of the main ridge (roughly delineated by the 2000 fm contour) and over an extensive area of the continental rise northeast of Cape Hatteras. Where y is present interpretation is made more difficult by its excellent reflecting characteristics which commonly prevent deeper reflectors from being seen. Reflector y appears occasionally to cut across bedding planes while maintaining its usual position about .6 sec below and parallel to the sea floor (Fig. 12 AB & EF). It is never clearly visible deeper than 5.5 sec below the water surface, a depth which corresponds, perhaps fortuitously, to the depth of principal change in calcium carbonate content (Peterson 1966).

Post x sedimentation is also complicated by the existence of the steeply-dipping reflector shown midway between the two ridges in Fig. 12

section AB and just to the right of the point where AB crosses on section EF. This reflector forms a plane with a dip of about 2° to the south. The plane, striking essentially east-west, has been observed only between 74°30' and 75°15'W, outcropping approximately along the 30°15'N latitude line. It is not present on the western flank of the southward extension of the main ridge (section CD); therefore it seems that unless this reflector is regarded as a fault plane, one of small throw and within the post x sequence, the post x evolution of the ridge may be considerably different to the north and south of latitude 30°15'N.

The ridge sediments above Horizon A both thin and dip gradually to the southeast along the ridge axis as shown in Fig. 14 (a structure section along the ridge axis derived from all available profiler crossings of the ridge crest). The sediments also thin and dip sharply to the east (from the axis) along the entire length of the ridge. On the west flank north of the "nose" the sediments have to a large degree filled in the area between the Escarpment and the ridge crest. This pattern of sediment thicknesses suggests the Blake Plateau as the principal sediment source for the construction of the Outer Ridge. This appears to be supported, at least for recent times, by the carbonate studies of Pratt & Heezen (1964) which indicate the Blake Plateau sediments as containing over 80% of carbonate material, the Blake Outer Ridge about 60%, the Blake-Bahama Basin 40-60%. North of Cape Hatteras the amount of calcium carbonate is small, rarely more than 3% (Stetson, 1939).

The two principal current systems available as media for transportation of sediment to the Outer Ridge are (1) the Florida Current, augmented by the Antilles Current, moving north and then turning northeast across the shallow Blake Plateau, and (2) the deep western boundary undercurrent which flows southward along the lower continental slope and upper continental rise in the vicinity of Cape Hatteras (Swallow & Worthington, 1961, and Barrett, 1965). Additional evidence for a source on the Blake Plateau is the presence of marked bottom scour on all echo sounder traverses across the axis of the Florida Current. This scour zone (Fig. 8) begins to widen at about 30°30'N where the combination of the gradual increase in bottom slope in the direction of the Blake Escarpment plus the coastal control exerted by the protrusion of the coast at Cape Hatteras induces a marked easterly component in the bottom current and scour patterns. The east-west "shoulder" at 31°N; 78-79°W also assists in promoting this tendency. Actual bottom current measurements (Pratt, 1963) indicate strong bottom currents of 25-40 cm/sec moving east and northeast at about 31°N;78°W. According to the bathymetry of reflector 4 (Ewing, J., et al, 1966), it seems probable that the principal flow in the past crossed the Escarpment slightly farther north, even nearer the root of the ridge than at present.

The existence of the two oppositely directed currents, together with the overall shape and structure of the Outer Ridge, suggests a mechanism for the formation of the ridge which is based on the assumption that the two currents interact to create the conditions necessary for the observed pattern of deposition. It is postulated that sediment-laden bottom water of the Florida Current, flowing roughly northeast, meets the undercurrent, flowing roughly southwest, at the edge of the Blake Plateau, both streams then being diverted to a generally southeast direction. The surface water of the Florida Current, passing over the undercurrent, continues northeast as the Gulf Stream. In the vicinity of the junction the interacting currents are slowed down and deposition takes place along the path of the resultant combined flow.

This picture is developed along quantitative lines in a separate note included as an appendix; the results obtained are in reasonable agreement with the main features of the depositional pattern. Since the major differential deposition occurred between Horizon A and reflector x (or possibly y), the model may not be as applicable to more recent sediments, including present day deposition. This would hardly be surprising since the model does not take into account the effect on the flow pattern of the changing topography as the ridge is being formed. In the limit the ridge would build up into the level of interaction and dominate the flow pattern. The original flow pattern may, of course, have been disturbed by processes unconnected with the building process itself, such as the previously mentioned possible southward shift of the region where the Florida Current bottom water leaves the Escarpment. A change of this sort would have a direct effect on the flow pattern and could explain the presence of the secondary ridge. In any case there are a number of secondary features which cannot be explained by the first order theory invoked here. Among these are the bench-like structures of Fig. 12 (EF), the related westward protrusion from the Outer Ridge at 30°30'N (well-displayed by the 1900 fm. contour), and the very sinusoidal periodic topography associated with some portions of the west flank of the secondary ridge (Figs. 3b and 12(AB)). A more exact hydrodynamic theory, coupled with more detailed knowledge of the boundary conditions, might explain some of these features; post-depositional slumping or other tectonic mechanisms might explain others, such as the aforementioned benches.

The question arises whether the two currents can in fact meet at the same level and interact as required. Estimates regarding the upper level of the undercurrent are conflicting but Barrett (1965) gives evidence that it is as shallow as 500 m at the inshore boundary near Cape Hatteras. Since the floor of the Blake Plateau is typically 800 m deep, considerable overlap would exist even if both currents were constrained by temperature stratification to remain at the respective levels dictated by the upstream boundary conditions. On the other hand, Swallow and Worthington suggest a figure of close to 2000 m for the top of the undercurrent farther south at about 33°N which would preclude any interaction if the streams remained in perfect thermal stratification. However, since the stream velocities are relatively high some disturbance of the stratification due to turbulence may be expected. Thus the sediment-laden bottom water of the Florida Current may in effect sink upon crossing the Escarpment, through the mechanism of downward turbulent transfer of both sediment and momentum. For sufficiently large sediment grains, gravitational settling could account for the sinking of the sediment even without eddy diffusion; the more important question is whether or not the eddy viscosity is large enough to effect the required momentum transfer against the temperature gradient.

Whatever the details of the interaction, and in spite of the many secondary aspects of the ridge structure which remain unexplained by this first order theory, the overall pattern of deposition is adequately explained in terms of the hydrodynamics of sediment-carrying currents.

Appendix: Hydrodynamic Model of the Formation of the Blake-Bahama Outer Ridge

G. M. Bryan

The proposed picture of the formation of the Blake-Bahama Outer Ridge by currents can be developed quantitatively on the basis of hydrodynamic theory. It is postulated that sediment-laden bottom water of the Florida Current, flowing roughly northeast, encounters the western boundary undercurrent, flowing roughly southwest, at the edge of the Blake Plateau, both streams then being diverted to a generally southeast direction. The surface water of the Florida Current, passing over the undercurrent, continues northeast as the Gulf Stream.

In the vicinity of the junction a hydrodynamically stable flow pattern can develop in which the flow velocity decreases to a minimum in the turn, then increases as the flow straightens out on the new course. If one or both of the streams is carrying sediment, deposition will take place in the region of lowered velocity, and the depositional pattern will be governed by the flow pattern. The relationship between flow pattern and depositional pattern will, in general, be quite complex and will depend to a large extent on the range of velocities and particle sizes involved. Relatively heavy particles, with settling velocities comparable to the flow velocities, will tend to deposit along isotachs corresponding to appropriate threshold velocities for deposition. On the other hand very light particles, which tend to stay in suspension for long periods of time, will tend to be distributed along streamlines, to the extent that they are deposited at all.

In order to proceed toward a quantitative theory it is necessary first to establish a reasonable flow pattern fitting the known boundary conditions and second to develop a suitable mechanism for deposition as a function of flow velocity and particle size. Both aspects of the problem require rather severe simplifying assumptions.

The hydrodynamic equations are usually linearized by a perturbation method in which the unperturbed solution represents the case of static equilibrium. First order perturbation for free steady motion with plane level surfaces and non-isentropic stratification then yields two-dimensional streamline flow of an incompressible fluid (see for example, Eckart, 1960). The first order velocity $\vec{v}$ then satisfies

$$\nabla \cdot \vec{v} = 0 \quad \text{and} \quad \vec{v} \cdot \nabla \chi = 0$$

where χ is the gravitational altitude.

In this approximation the flow is also irrotational and the methods of potential theory are applicable. In particular for two-dimensional motion we introduce the complex potential

$$W(z) = \phi + i\,\psi$$

where $z = x + iy$ and the velocity potential ϕ and the stream function χ are conjugate solutions of Laplace's equation.

Writing for the velocity $\vec{v} = v_x + i v_y = q\, e^{i\theta}$ we have,

$$v_x = -\frac{\partial \phi}{\partial x} = -\frac{\partial \psi}{\partial y} \quad \text{and} \quad v_y = -\frac{\partial \phi}{\partial y} = \frac{\partial \psi}{\partial x}$$

from which it follows that

$$v^* = -\frac{dW}{dz}$$

where $v^* = qe^{-i\theta}$ is the complex conjugate of the flow velocity.

In Fig. 15a the x-axis is a rigid boundary representing the Blake Escarpment from Cape Hatteras on the left to about latitude 30°30'N on the right. Two streams of widths w_1 and $w_2 < w_1$, following the boundary, meet at the origin and are diverted to a new direction. This problem is equivalent to that shown in Fig. 15b in which two streams of widths $2w_1$ and $2w_2$ meet head on without the influence of rigid boundaries. The line of symetry in Fig. 15b can be replaced with a rigid wall to give the problem of Fig. 15a. The problem of impinging streams in two dimensions has been treated in considerable detail in classical hydrodynamics (see for example Milne-Thompson, 1955, chapter XI). A stationary flow pattern requires that the two streams have the same speed at infinity, and this is assumed without further justification. The complex velocity $v = qe^{i\theta}$ is then related to the position $z = x + iy$ by

$$z = \frac{1}{\pi}\left\{2w_1 \ln\left(1 - \frac{v^*}{U}\right) - 2w_2 \ln\left(1 + \frac{v^*}{U}\right) - (w_1 + w_2)\, e^{i\beta} \ln\left(1 - \frac{v^*}{U} e^{i\beta}\right) - (w_1 + w_2)\, e^{-i\beta} \ln\left(1 - \frac{v^*}{U} e^{-i\beta}\right)\right\}$$

where U = upstream speed at infinity, β = asymptotic direction of final flow. An isotach is the locus of z traced out by varying θ at fixed q. The complex potential W, whose imaginary part is the stream function, is also most easily expressed in terms of v^* :

$$W = \frac{U}{\pi}\left\{2w_1 \ln\left(1 - \frac{v^*}{U}\right) + 2w_2 \ln\left(1 + \frac{v^*}{U}\right) - (w_1 + w_2) \ln\left(1 - \frac{v^*}{U} e^{i\beta}\right) - (w_1 + w_2) \ln\left(1 - \frac{v^*}{U} e^{-i\beta}\right)\right\}$$

The final flow direction is related to the initial upstream widths at infinity by

$$\cos \beta = \frac{w_1 - w_2}{w_1 + w_2}$$

and the final downstream width of the combined flow is $w\beta = w_1 + w_2$.

If the widths and velocities of the two streams were known the final flow direction β could be computed and isotachs and streamlines mapped in the x,y plane. In the present case the parameters of the incoming streams are not that well known; the angle β was inferred from the known topography and used to compute isotachs and streamlines in dimensionless form. The resulting patterns were then adjusted in scale to fit the topography, after which the stream widths could be predicted. (Since we are assuming deposition on a nearly level Horizon A, the topographic contours correspond approximately to isopachs.)

The streamlines and isotachs computed for $\beta = 66^\circ$ are shown in dimensionless form in Fig. 16. There is a stagnation point at the origin, where the streamlines coincident with the boundary change direction discontinuously as the flow velocity vanishes. A dividing streamline, which marks the boundary between the two bodies of fluid in the combined flow, is perpendicular to the rigid boundary at the stagnation point, curves downstream away from the wid current, and approaches asymptotically the final flow direction β . Velocity is continuous across this dividing streamline; the isotachs approach concentric circles about the stagnation point at the low velocity limit and approach the streamlines as the velocity approaches the upstream velocity U. The outer edges of the flow constitute free streamlines with constant velocity U. The isotachs in

Fig. 16 are plotted at velocity intervals of 0.1U.

In Fig. 17 the flow pattern is compared with the bathymetry of the ridge, the scale having been adjusted to obtain the best fit between the dividing streamline and the ridge axis. The resulting stream widths are 74 km on the north, 31 km on the south and 105 km for the combined downstream flow. Available experimental determinations of the undercurrent are variable and sometimes show considerable structure. According to Barrett (1965) the width off Cape Hatteras is probably between 20 and 80 km. Farther south ($\sim 33^{\circ}$N) Swallow and Worthington (1961) show several sections with peak velocities in the range of 10-18 cm/sec and widths of 90-100 km to the 1 cm/sec points at the bottom. Still farther south ($\sim 32^{\circ}30'$N), and well into the pattern of converging streams, their Section I shows peak velocity down to about 7 cm/sec and stream width more than doubled.

Similarly detailed measurements do not seem to be available for the Florida Current in the neighborhood of the current junction. For what it is worth, however, the scour pattern on the Blake Plateau just north of the Florida Straits is about 30 km wide, in reasonable agreement with the predicted upstream width of 31 km.

Further support for the hydrodynamic model is found in the close fit between the curving ridge crest and the dividing streamline of the flow pattern, along which maximum deposition should take place. The crest appears to divide the ridge into two distinct depositional regimes: on the east flank the topographic contours are nearly parallel to the crest, tending to follow the streamlines of the flow pattern (Fig. 17) while on the west the contours make large angles with the crest and tend to follow isotachs (Fig. 18). As discussed qualitatively above, this suggests that relatively fine sediment is moving south in the undercurrent, and relatively coarse sediment is coming north in the Florida Current.

ACKNOWLEDGMENTS

This work was supported by the U. S. Navy under Contract NObsr 85077 with the Bureau of Ships. This publication is for technical information only and does not represent recommendations or conclusions of the sponsoring agency. Reproduction of this document in whole or in part is permitted for any purpose of the United States Government.

The authors wish to acknowledge many helpful discussions with J. Ewing and R. Houtz as well as the contributions of the many Lamont personnel involved in obtaining the data at sea.

The cooperation of the staff of Hudson Laboratories of Columbia University in making available their flow camera facilities is gratefully acknowledged.

The investigation of microtopography grew out of work performed in cooperation with H. Weaver and J. Geary of the U. S. Navy Underwater Sound Laboratory.

REFERENCES

Barr :tt, J. R., Jr., Subsurface currents off Cape Hatteras; Deep Sea Research, v. 12, p. 173-184 (1965)

Bryan, G. M., Proceedings of Seminar on Reflection of Sound by the Ocean Bottom; USNUSL, May 25, 26 (1964)

Bryan, G. M. and J. Ewing, Proceedings of the 22nd U.S. Navy Symposium on Underwater Acoustics; October 26-28 (1964)

Clay, C.S. and P. A. Rona, On the existence of bottom corrugations in the Blake-Bahama Basin; Journal of Geophysical Research, v.69, No. 2, P. 231-234 (1964)

Eckert, C., Hydrodynamics of Oceans and Atmospheres, Pergamon Press Inc., New York (1960)

Ewing, J., M. Ewing and R. Leyden, Seismic-Profiler Survey of Blake Plateau; Am. Assoc. Petroleum Geologists Bull., v 50, No. 9, p. 1948-1971 (1966)

Ewing, J., J. L. Worzel, M. Ewing, C. Windisch, Ages of Horizon A and the Oldest Atlantic sediments; Science, v. 154, No. 3753, p. 1125-1132 (1966)

Ewing, M., and J. Ewing, Distribution of oceanic sediments; Studies on Oceanography, p. 525-537 (1964)

Luskin, B., J. E. Nafe and M. Ewing, The Use of Topographic Highlights for the Measurement of Ship's Ground Speed; TR No. 15 (CU-41-57-NObsr 64547-Geol.)(1957)

Milne-Thompson, L. M., "Theoretical Hydrodynamics", 3rd Edition, Macmillan Co., New York (1955)

Officer, C. B., "Introduction to the Theory of Sound Transmission" McGraw-Hill Co., New York (1958)

Peterson, M. N. A., Calcite: Rates of dissolution in a vertical profile in the central Pacific; Science, v. 154, No. 3756, p. 1542-1544 (1966)

Pratt, R. M., Bottom currents on the Blake Plateau; Deep Sea Res., v. 10, p. 245-249 (1963)

Pratt, R. M. and B. C. Heezen, Topography of the Blake Plateau; Deep Sea Res., v. 11, p. 721-728 (1964)

Stetson, H.C., Summary of Sedimentary conditions on the continental shelf off the east coast of the U. S. in "Recent Marine Sediments", P. D. Trask, Ed., p. 230-244 (1939)

Swallow, J.C. and L. V. Worthington, An observation of a deep counter-current in the Western North Atlantic; Deep Sea Res., v. 8, p. 1-19 (1961)

Weaver, H. R., Proceedings of Seminar on Reflection of Sound by the Ocean Bottom; USNUSL, May 25, 26 (1964)

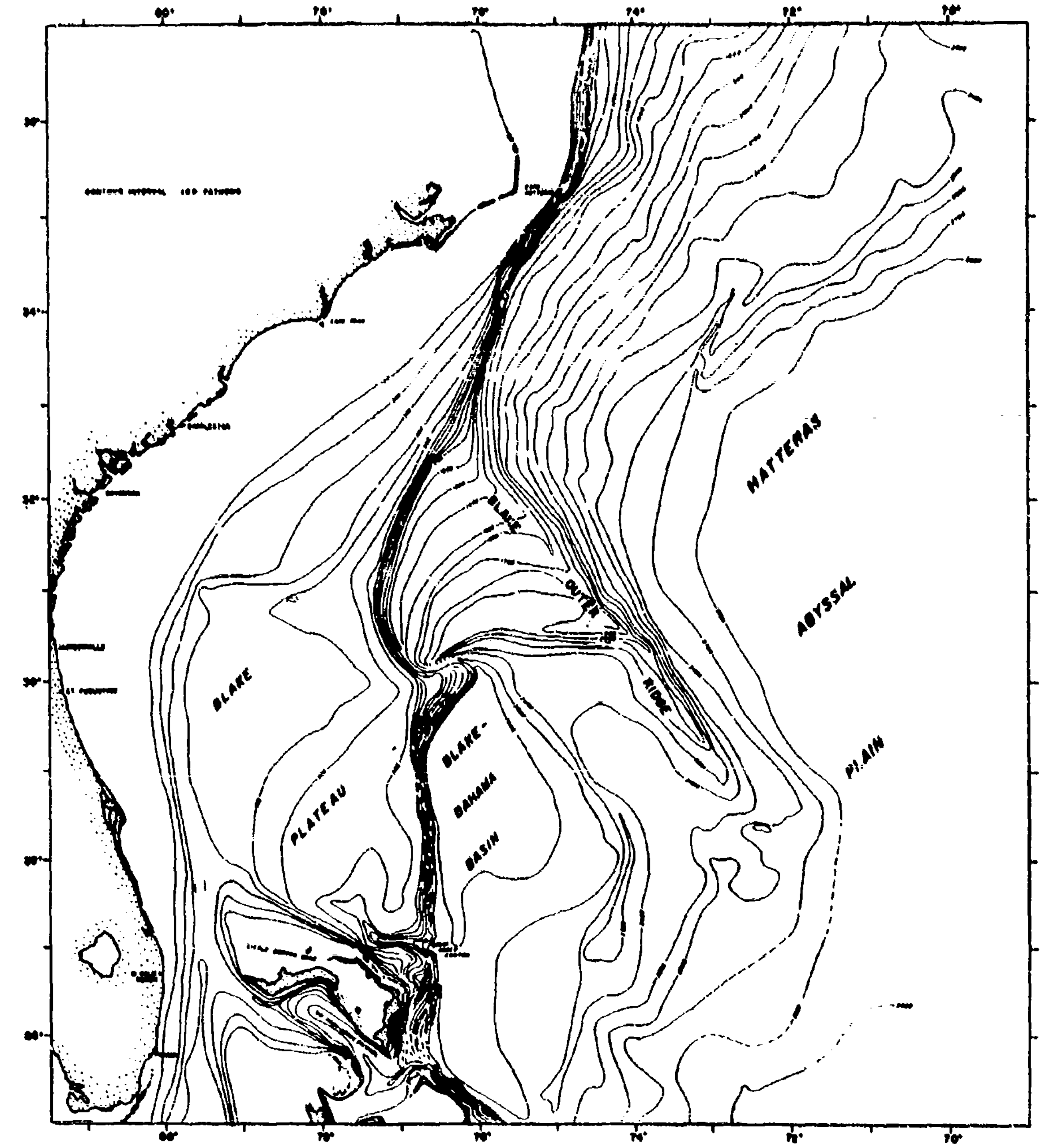

Fig. 1. Bathymetric and province map of the Blake-Bahama region.

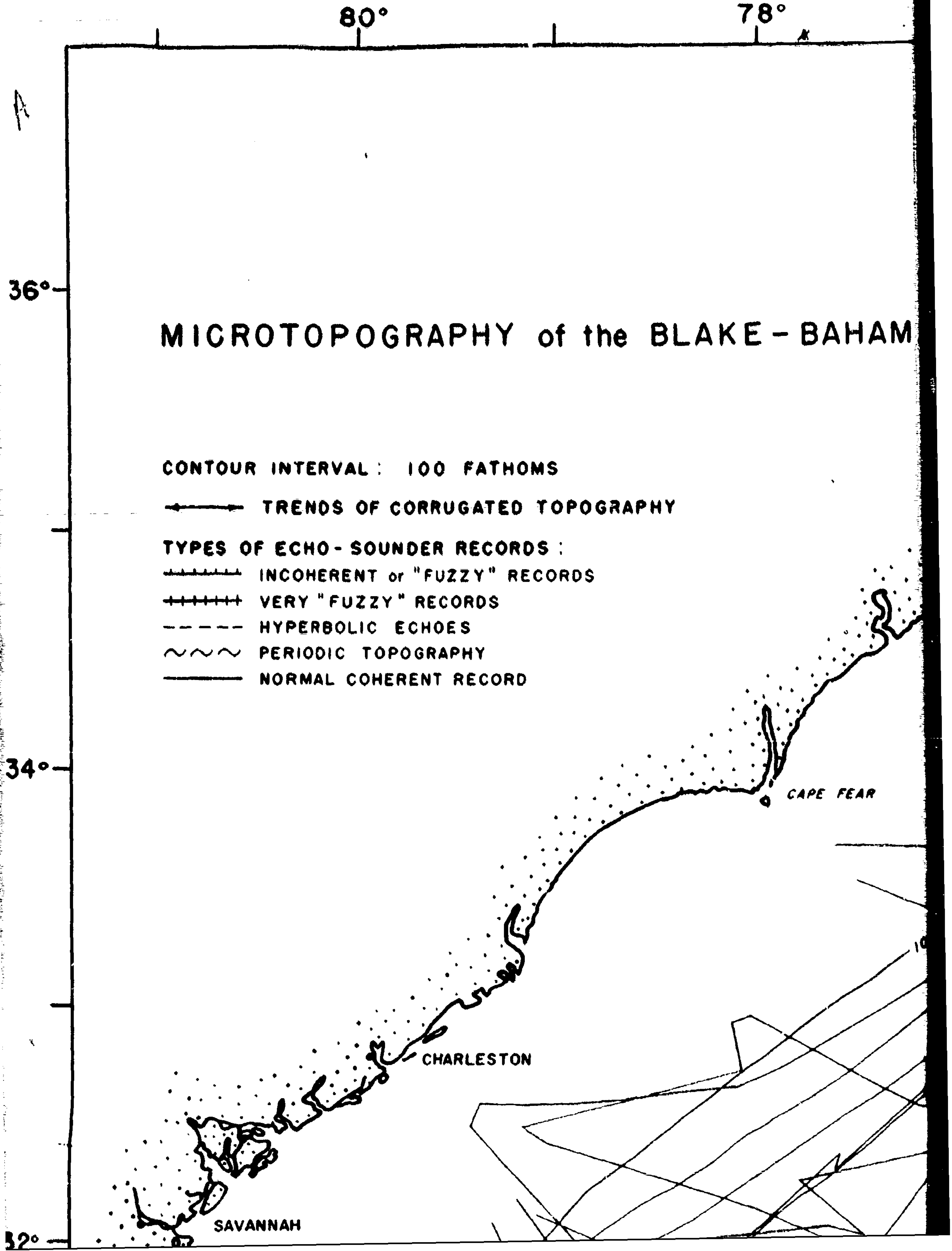
80°
78°
36°
34°
32°
MICROTOPOGRAPHY of the BLAKE - BAHAM
CONTOUR INTERVAL : 100 FATHOMS
TRENDS OF CORRUGATED TOPOGRAPHY
TYPES OF ECHO - SOUNDER RECORDS :
INCOHERENT or "FUZZY" RECORDS
VERY "FUZZY" RECORDS
HYPERBOLIC ECHOES
PERIODIC TOPOGRAPHY
NORMAL COHERENT RECORD
CAPE FEAR
CHARLESTON
SAVANNAH

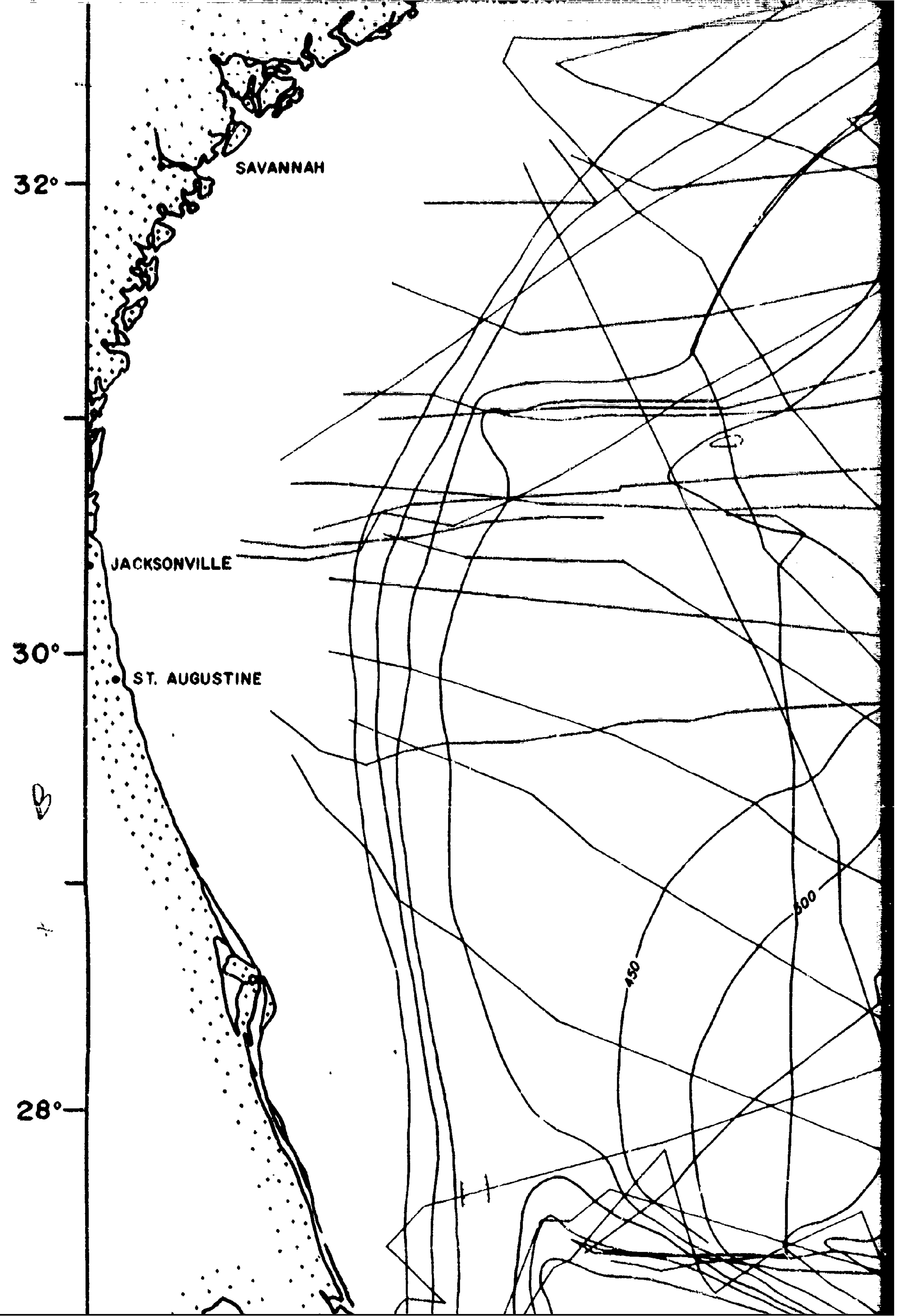

32°
SAVANNAH
JACKSONVILLE
30°
ST. AUGUSTINE
28°
450
500

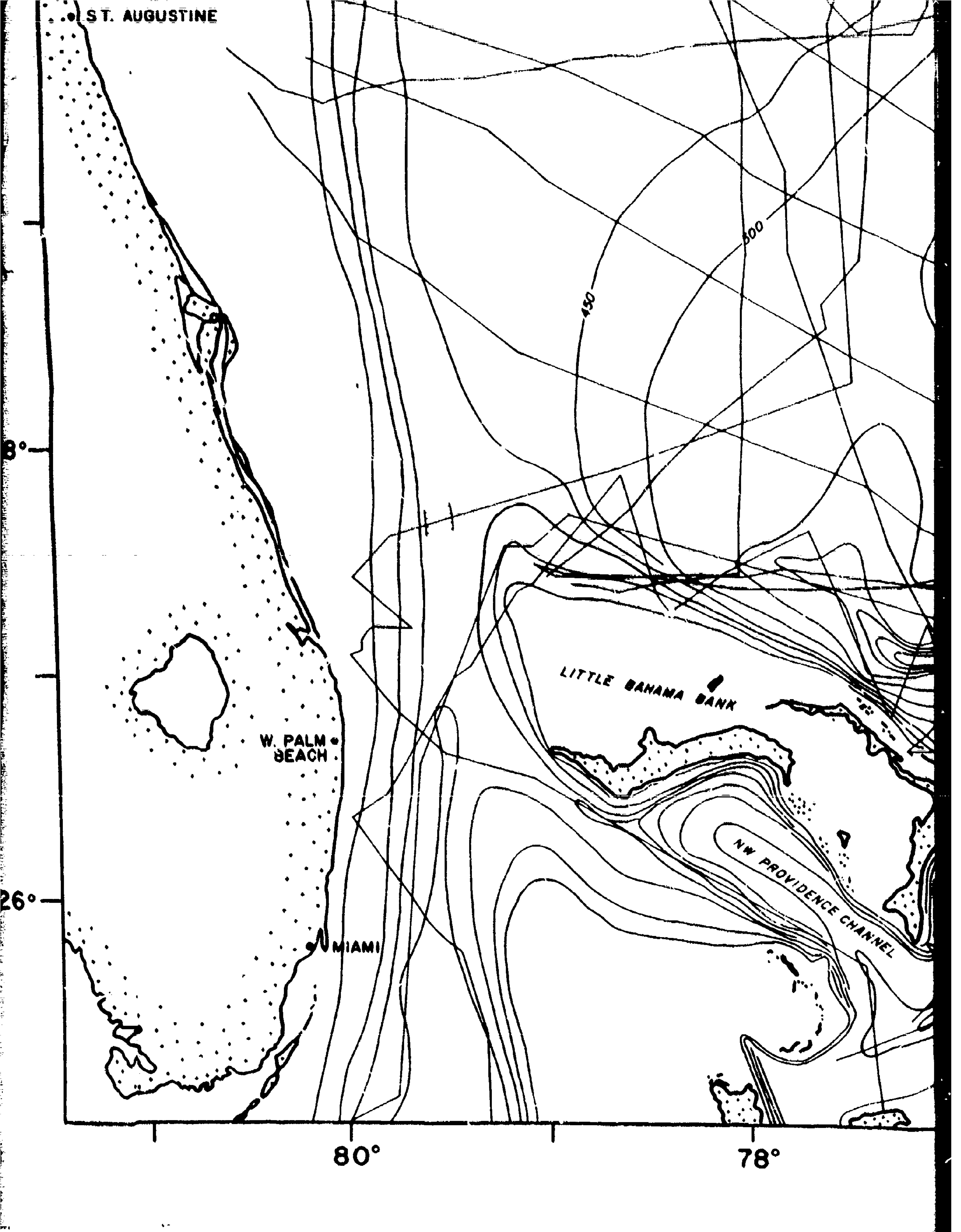

ST. AUGUSTINE
28°
26°
W. PALM BEACH
MIAMI
LITTLE BAHAMA BANK
NW PROVIDENCE CHANNEL
450
500
80°
78°

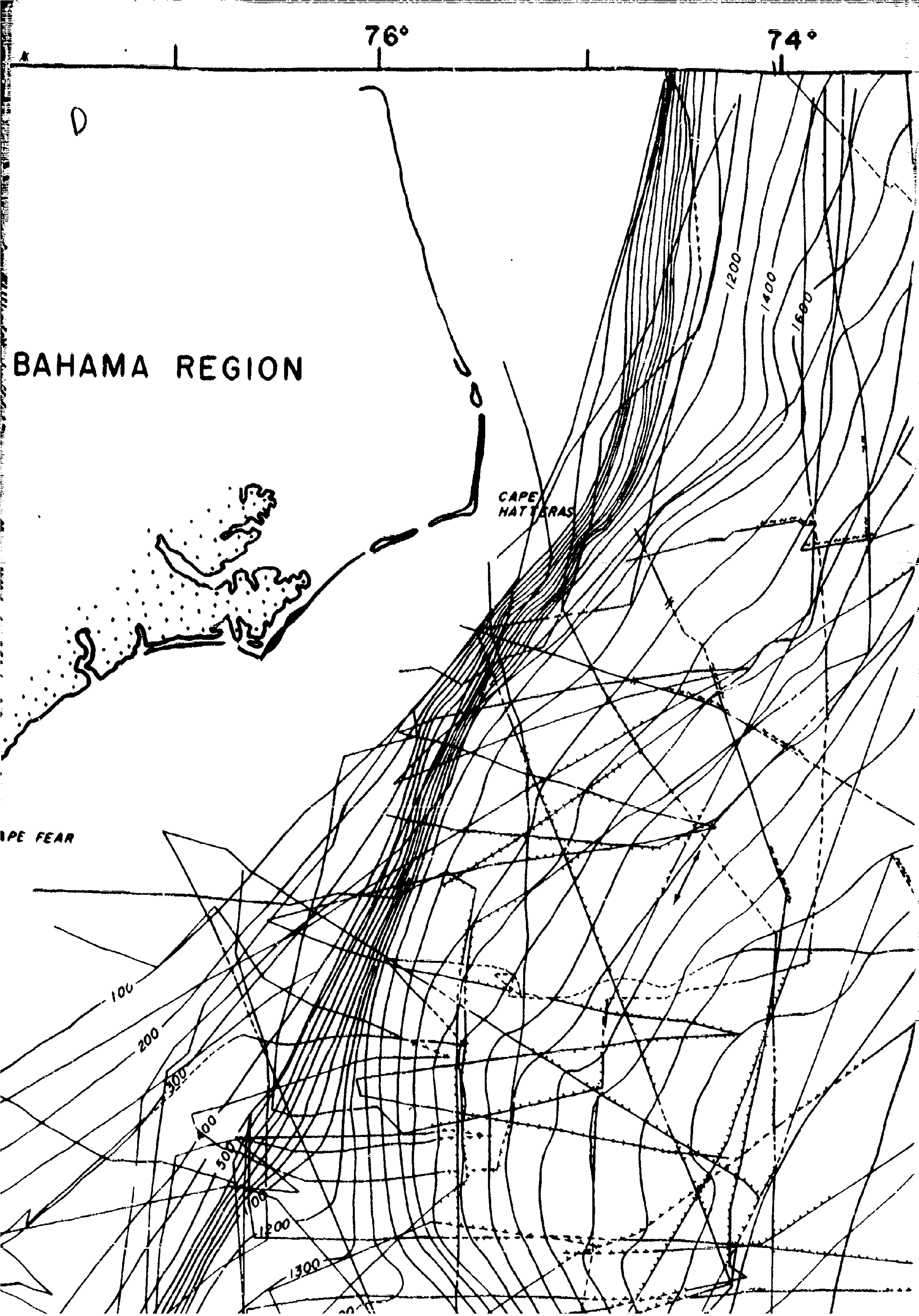
76°
74°
D
BAHAMA REGION
CAPE HATTERAS
APE FEAR
100
200
300
400
500
1100
1200
1300
1200
1400
1600

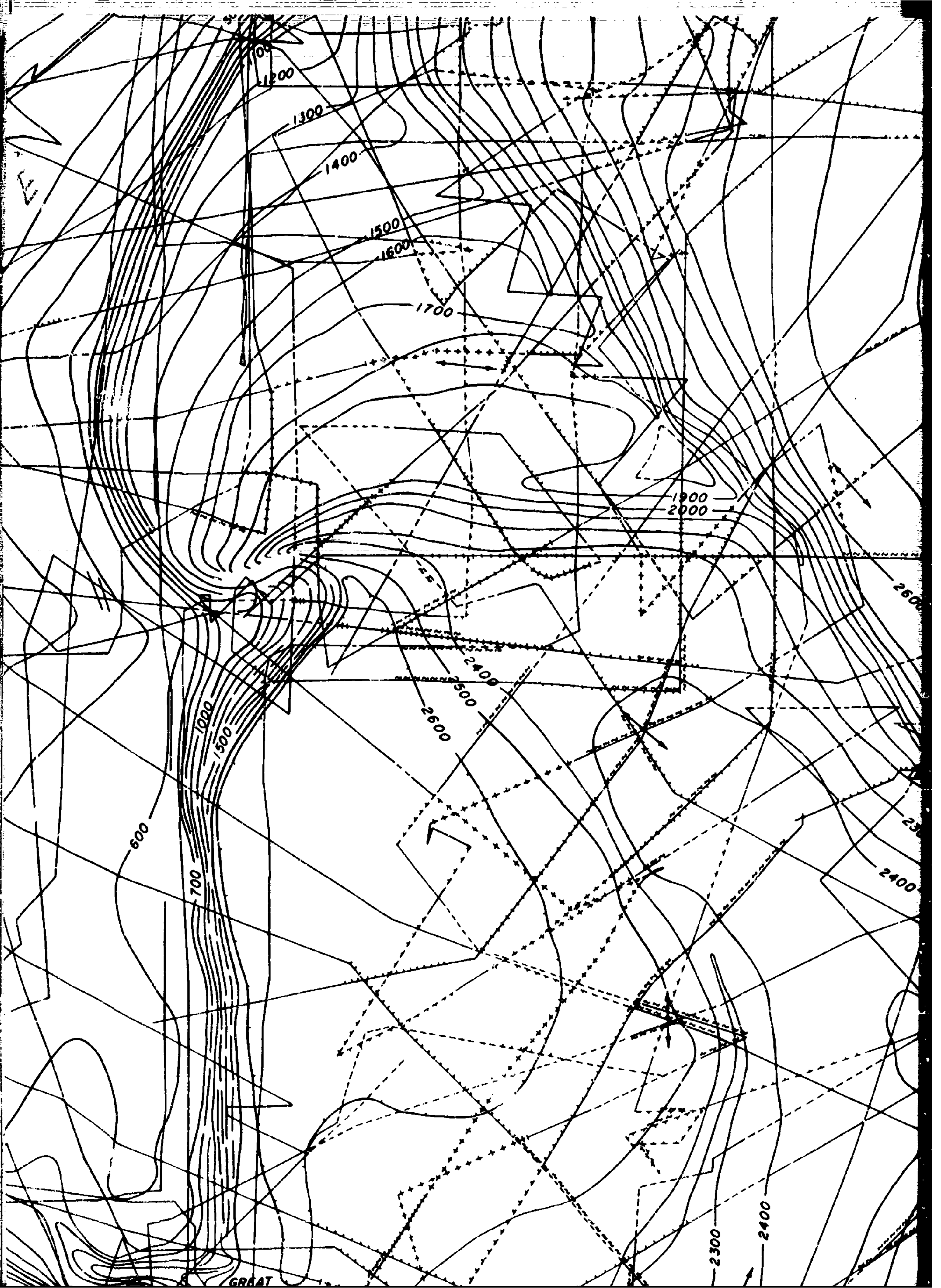

1100
1200
1300
1400
1500
1600
1700
1900
2000
2400
2500
2600
1000
1500
600
700
2400
2300
2400
GREAT

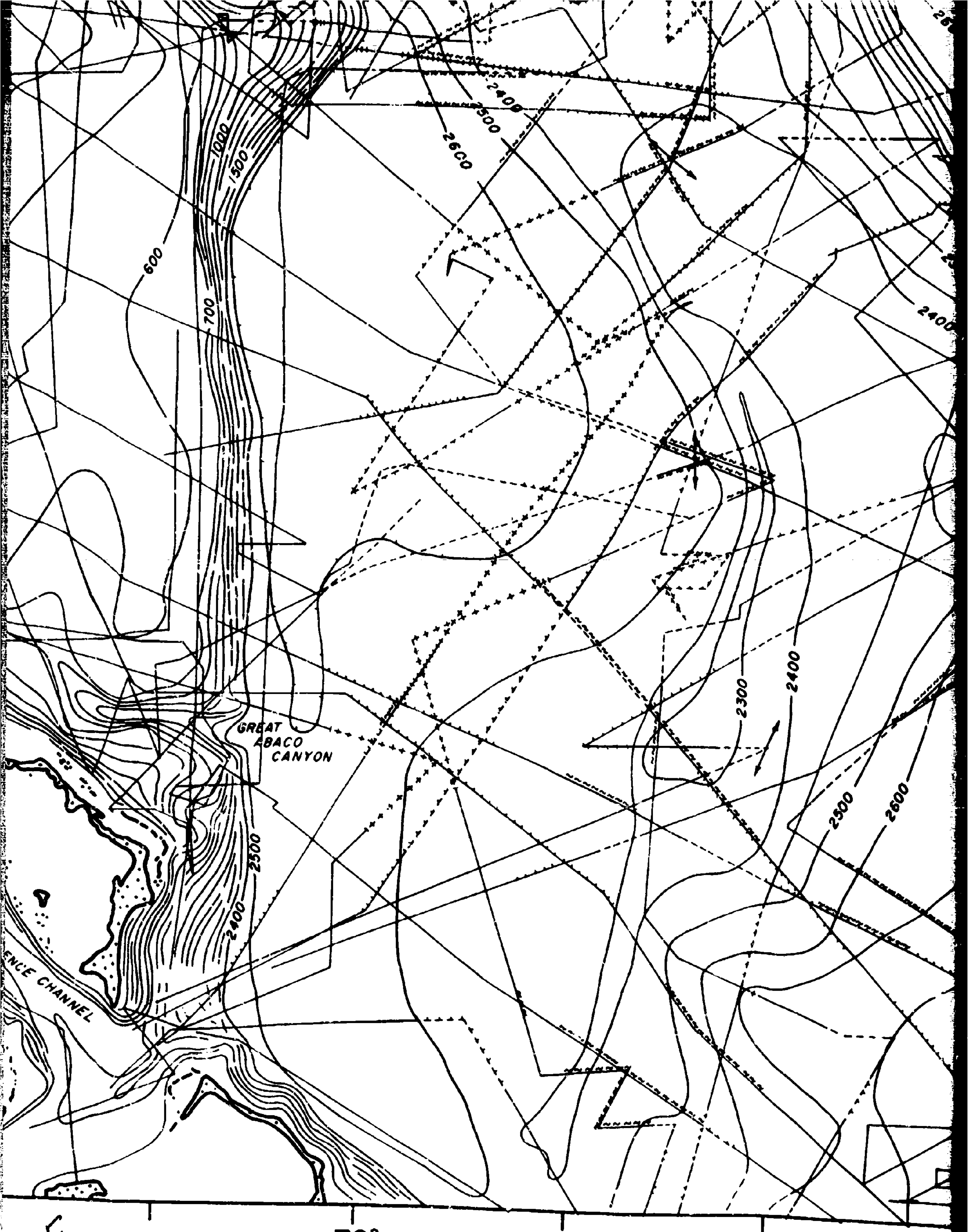

GREAT
ABACO
CANYON
ENCE CHANNEL
600
700
1000
1500
2300
2400
2500
2600
76°
74°

F

72°
70°
G
2300
1800
1900
2000
2100
2200
2400
2500
2600
2700
2800

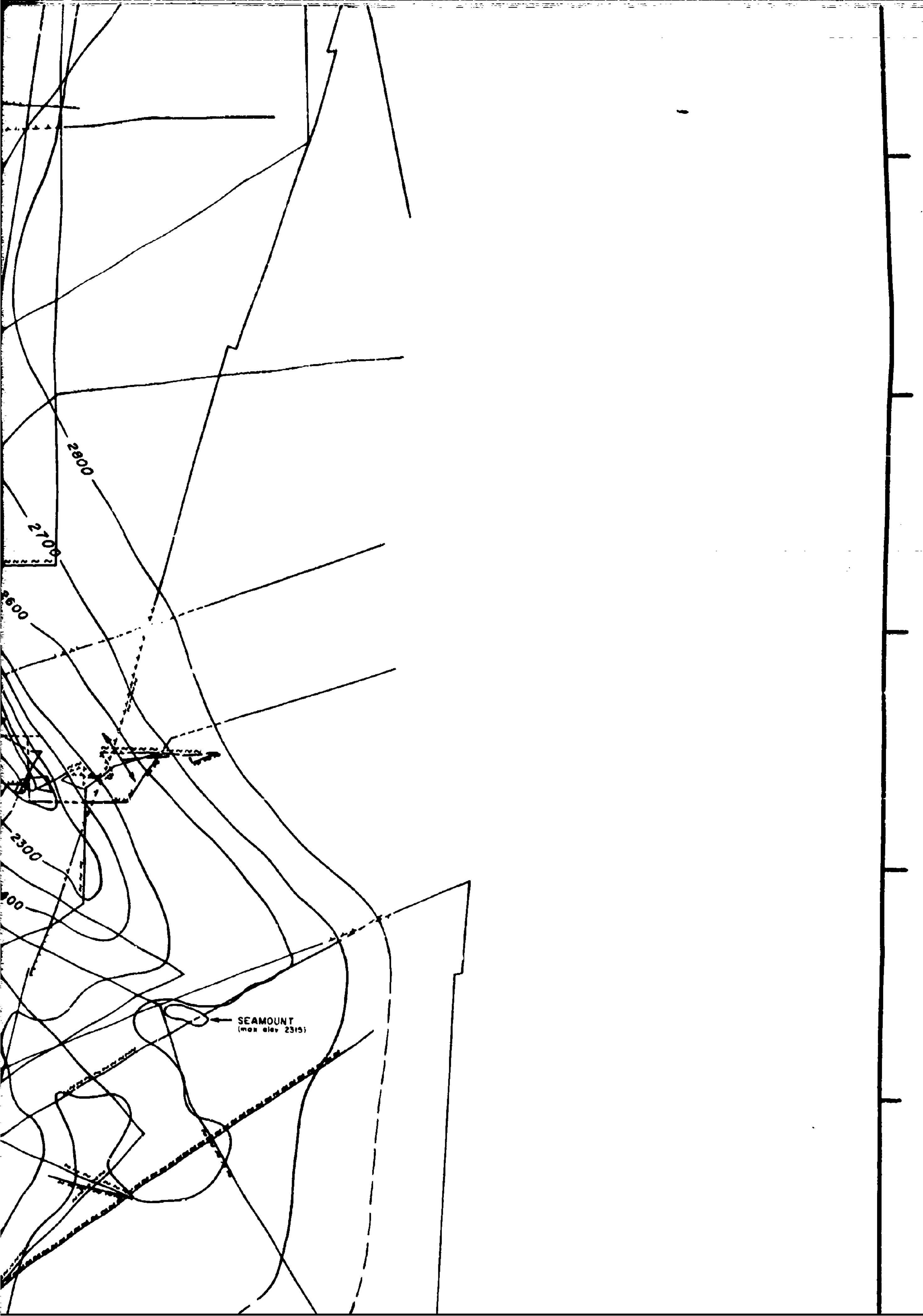
2800
2700
2600
2300
SEAMOUNT
(max elev 2315)

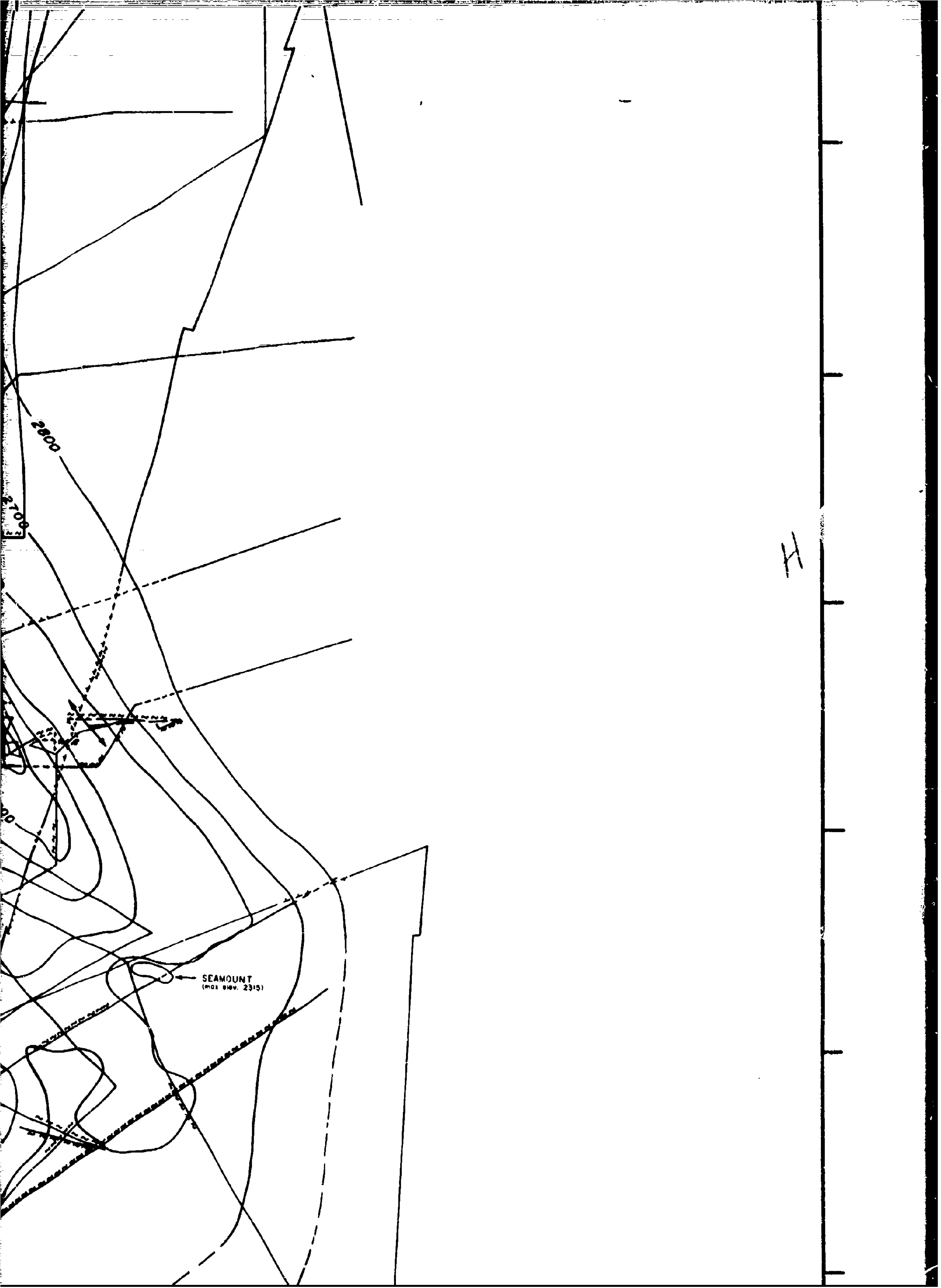

2800
2700
SEAMOUNT
(max elev. 2315)
H

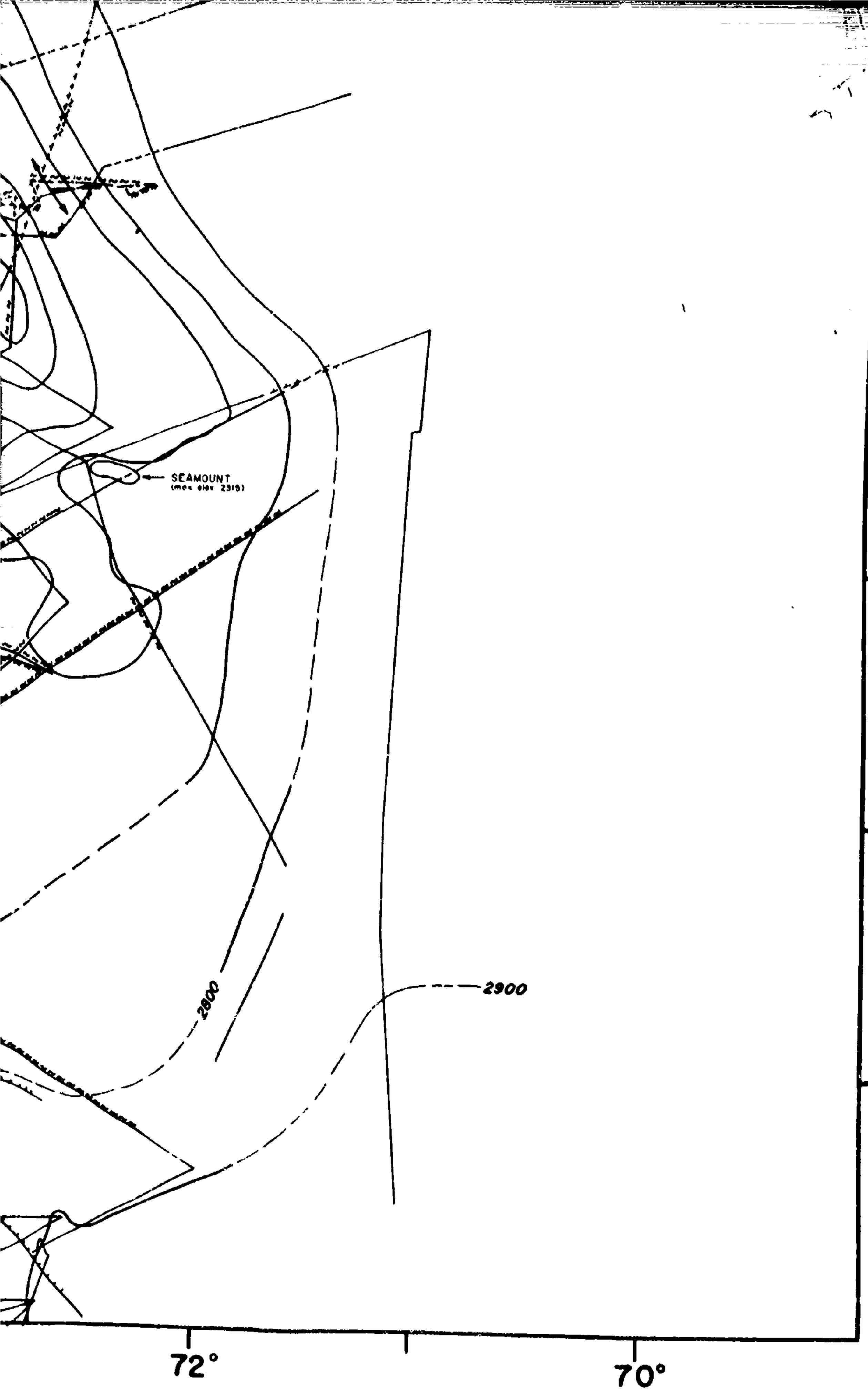
SEAMOUNT
(max elev 2319)
2800
2900
72°
70°

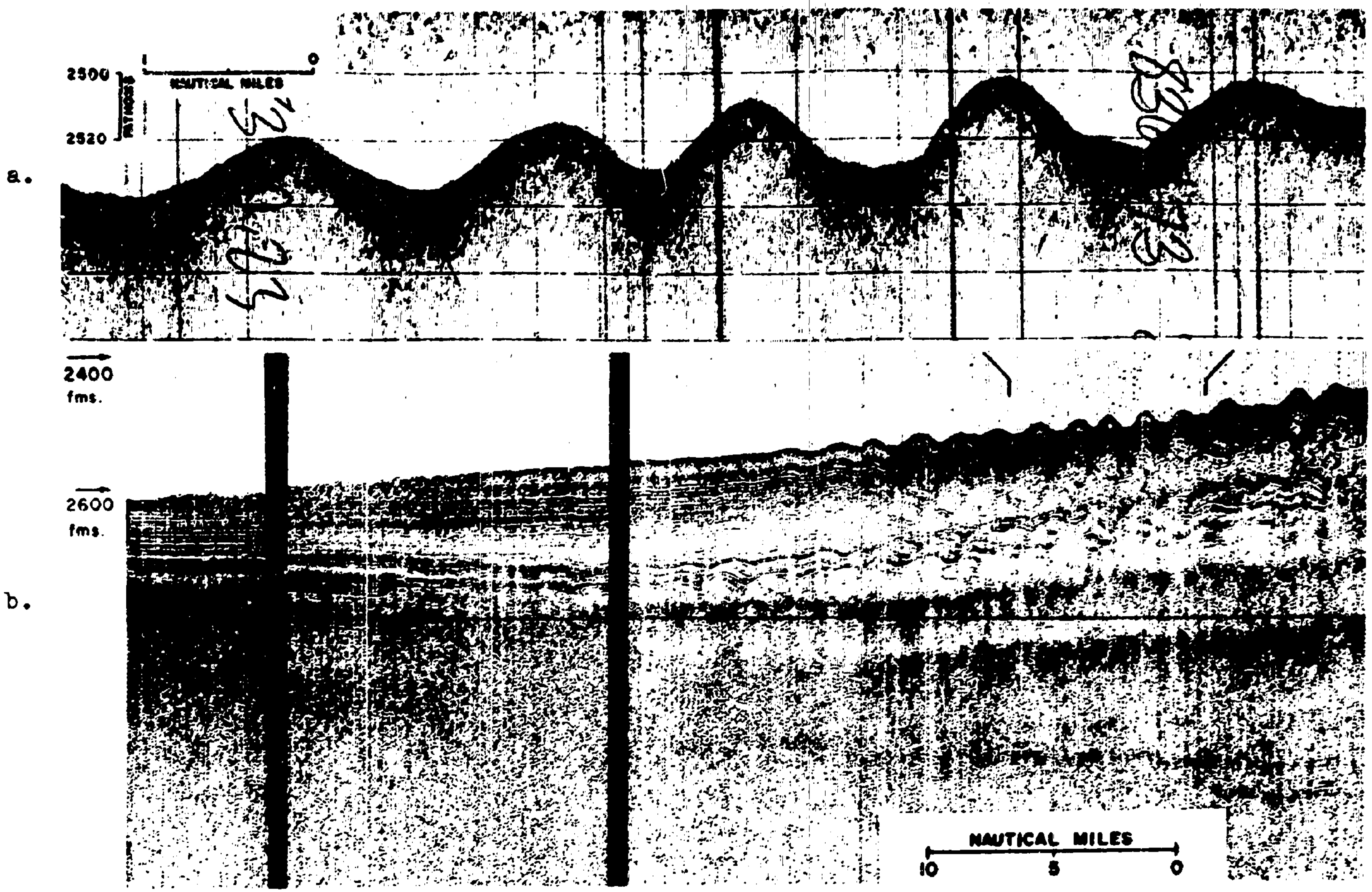

Fig. 3. Very sinusoidal periodic topography. (a.) a portion of PDR trace made simultaneously with b. (b.) a seismic reflection profile.

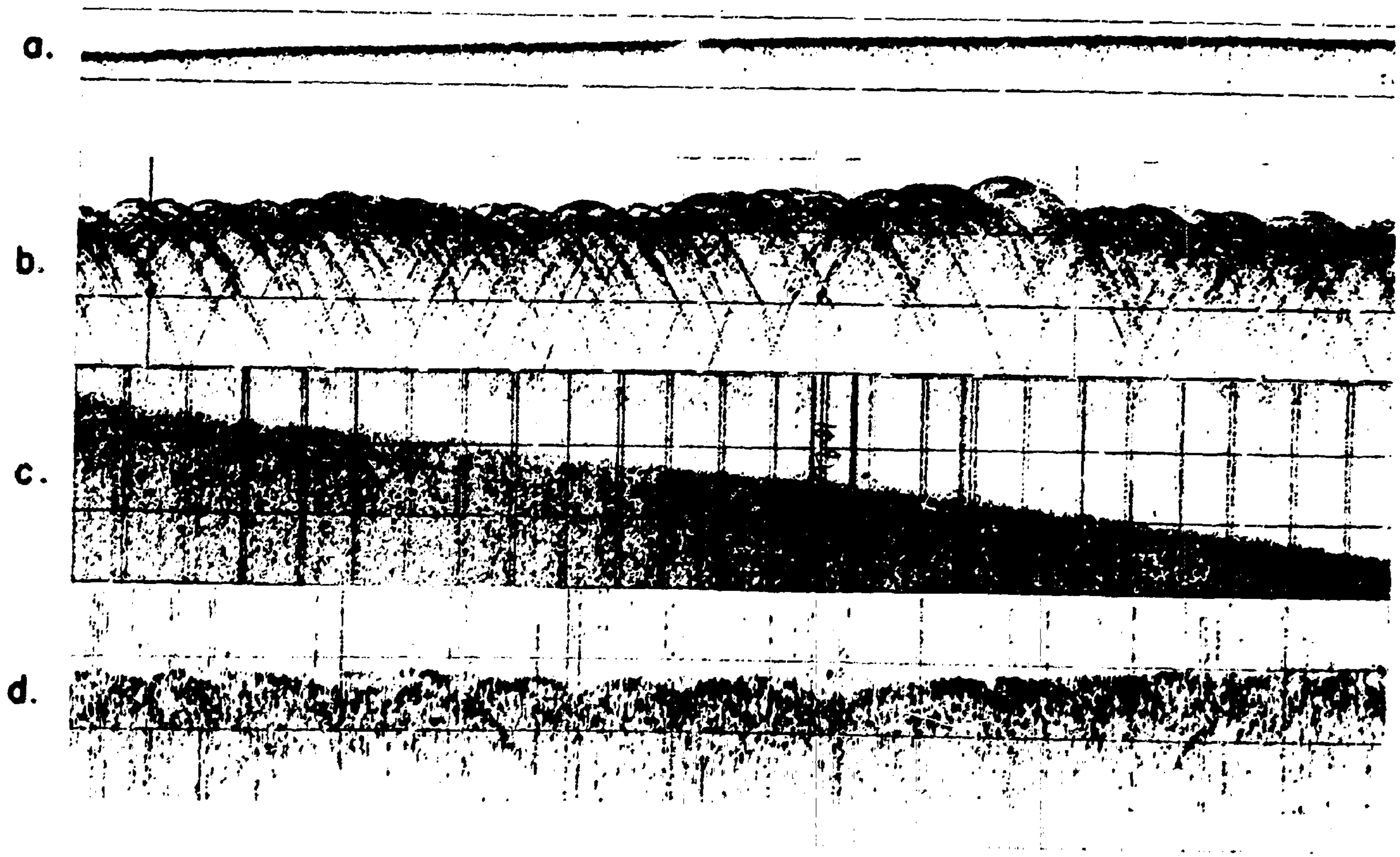

Fig. 4. Types of echo sounder trace: a. coherent record b. hyperbolic echoes c. incoherent or "fuzzy" record d. fuzzy hyperbolic echoes.

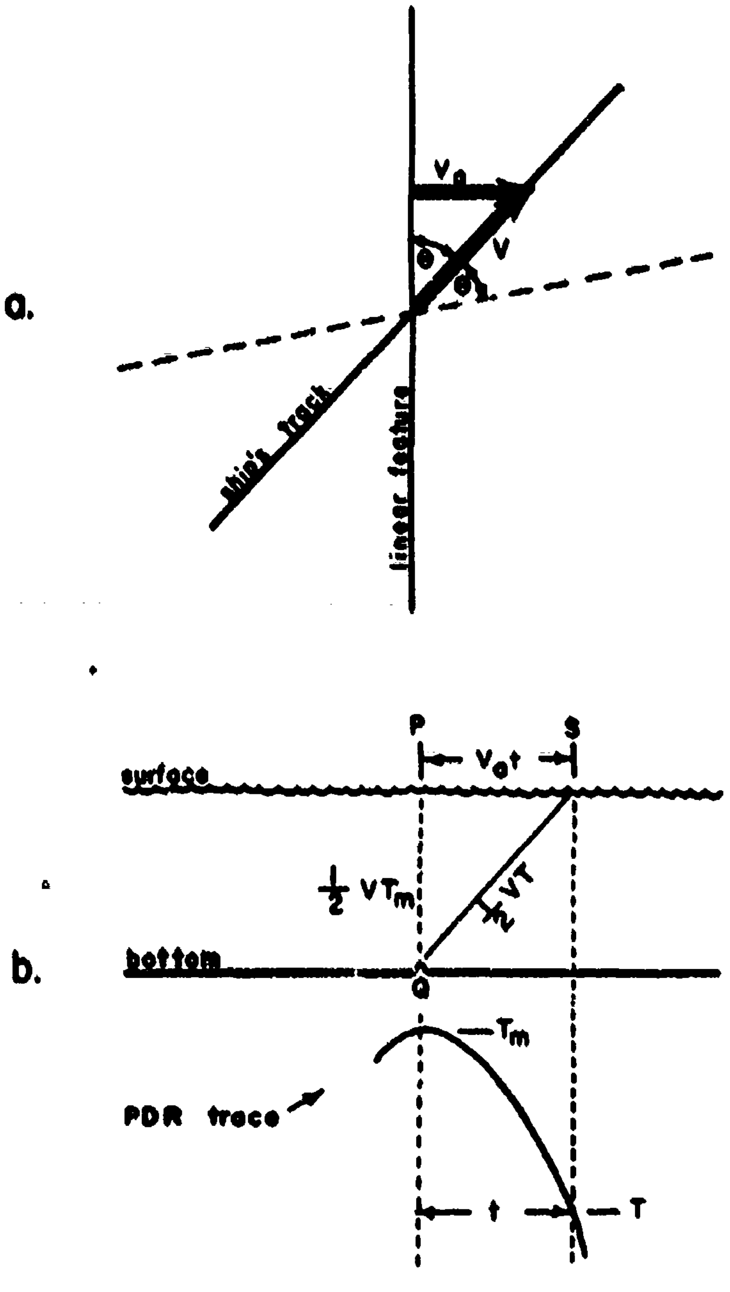

Fig. 5. Construction of hyperbolic echo assuming a linear feature.

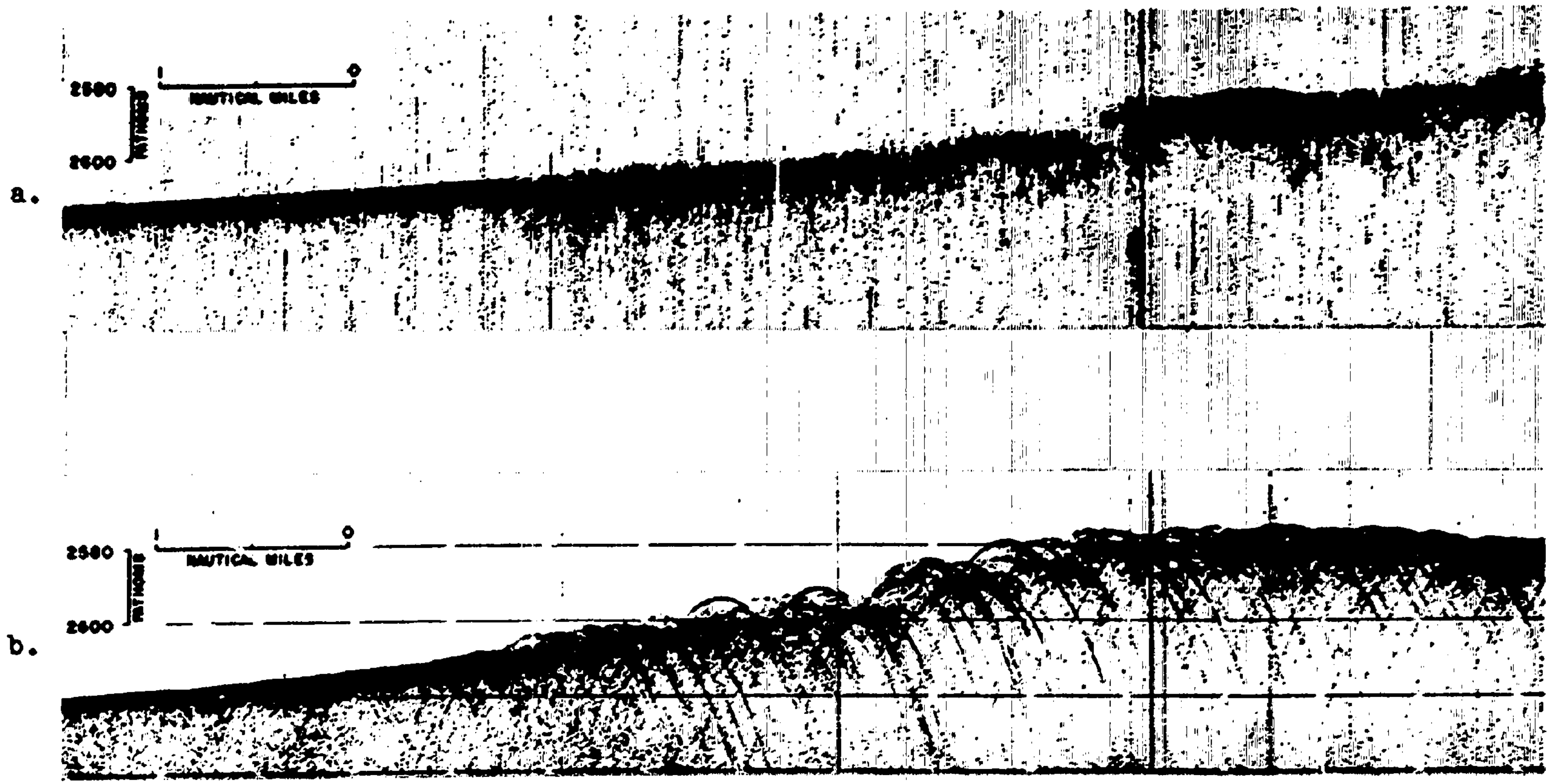

Fig. 6. Typical sharp transition from coherent to incoherent echo sounder trace.
a. long ping length
b. short ping length

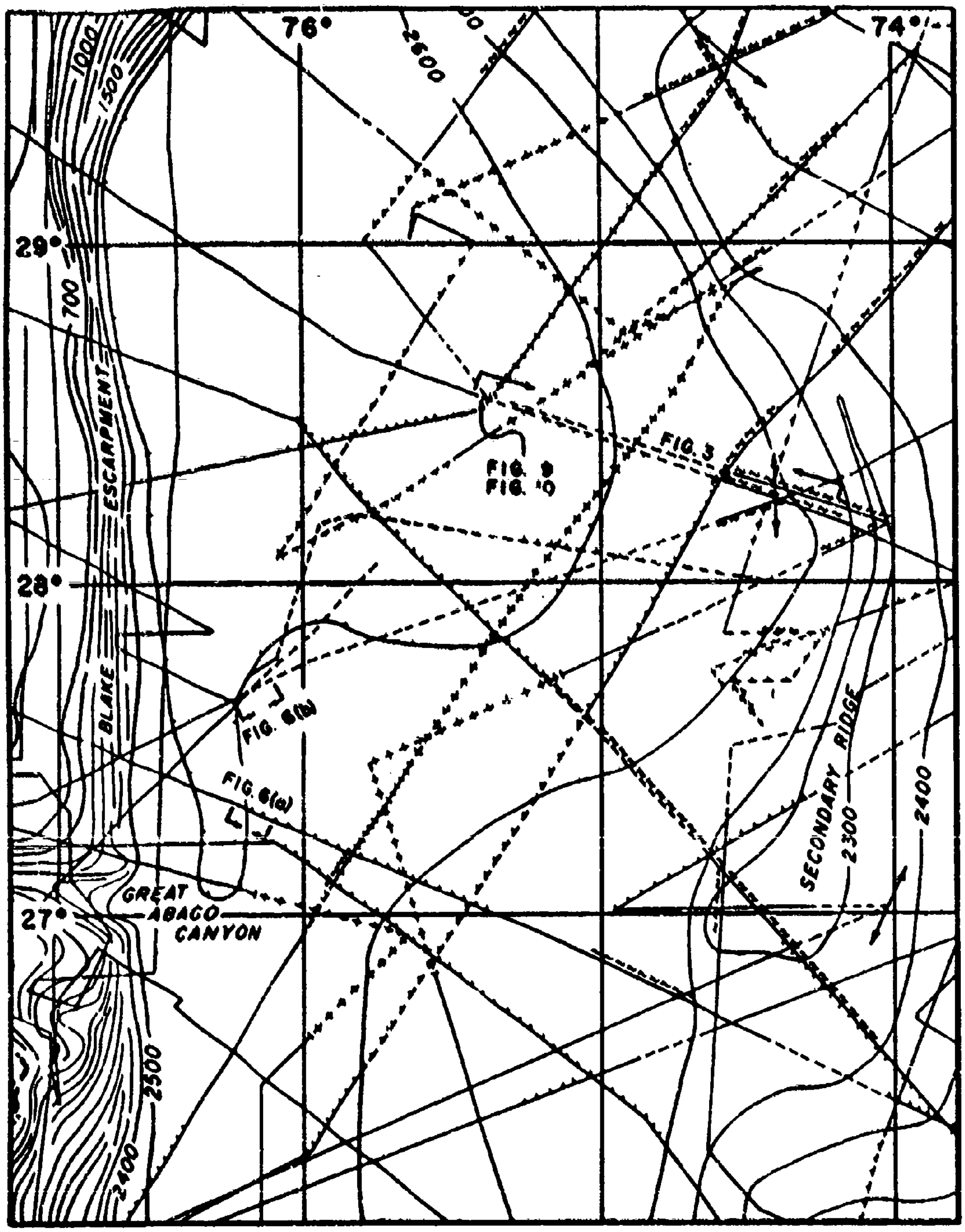

Fig. 7. Location map for Figures 3, 6, 9, and 10.

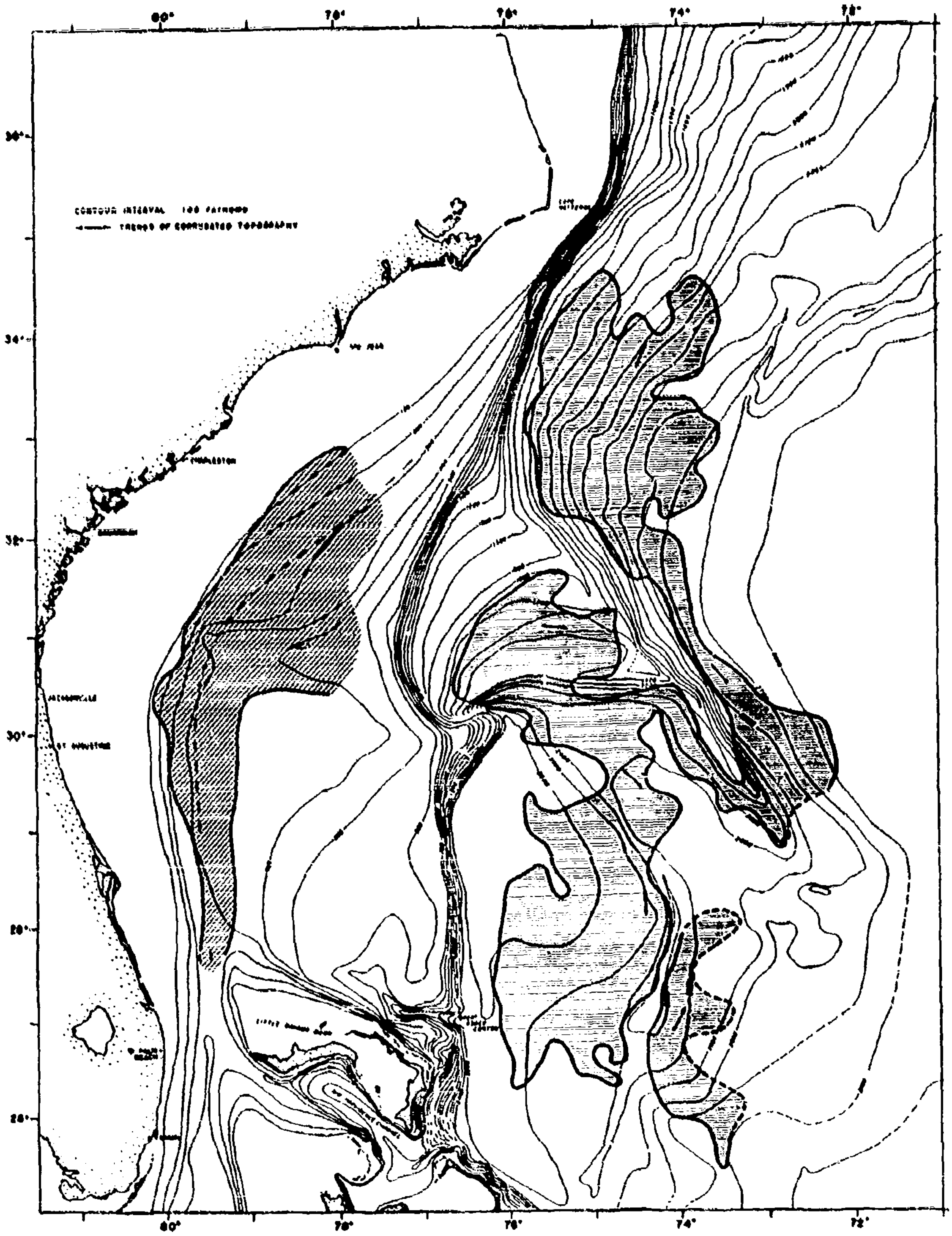

Fig. 8 Outline of the area exhibiting fuzzy and hyperbolic PDR traces caused by microtopography. The axis of the Florida Current and the zone of scoured bottom on the Blake Plateau are also indicated.

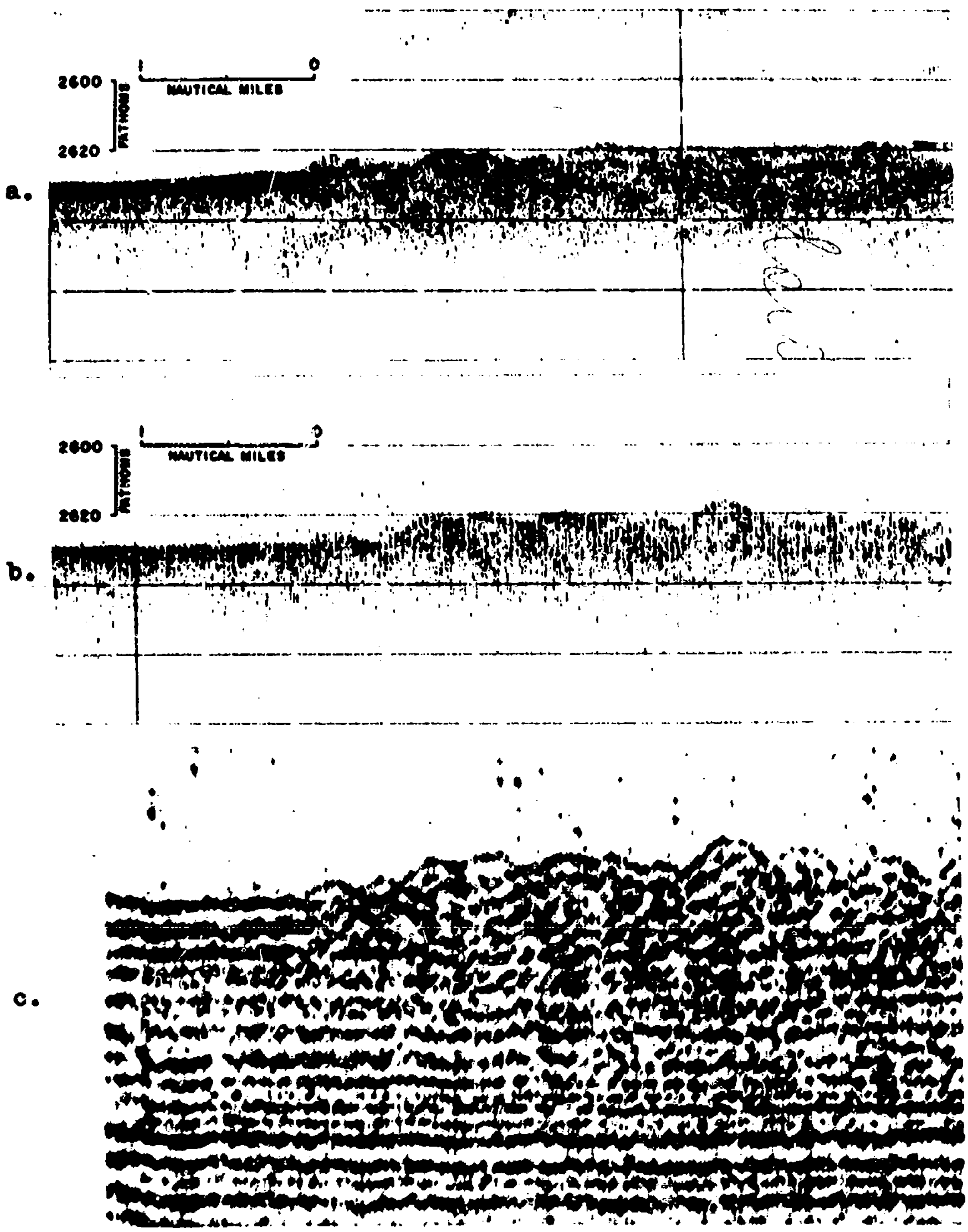

Fig. 9. Typical sharp transition from coherent to hyperbolic echo trace. (a.) ungated PDR (b.) gated PDR trace made simultaneously with c. (c.) an enlarged section of seismic profile record.

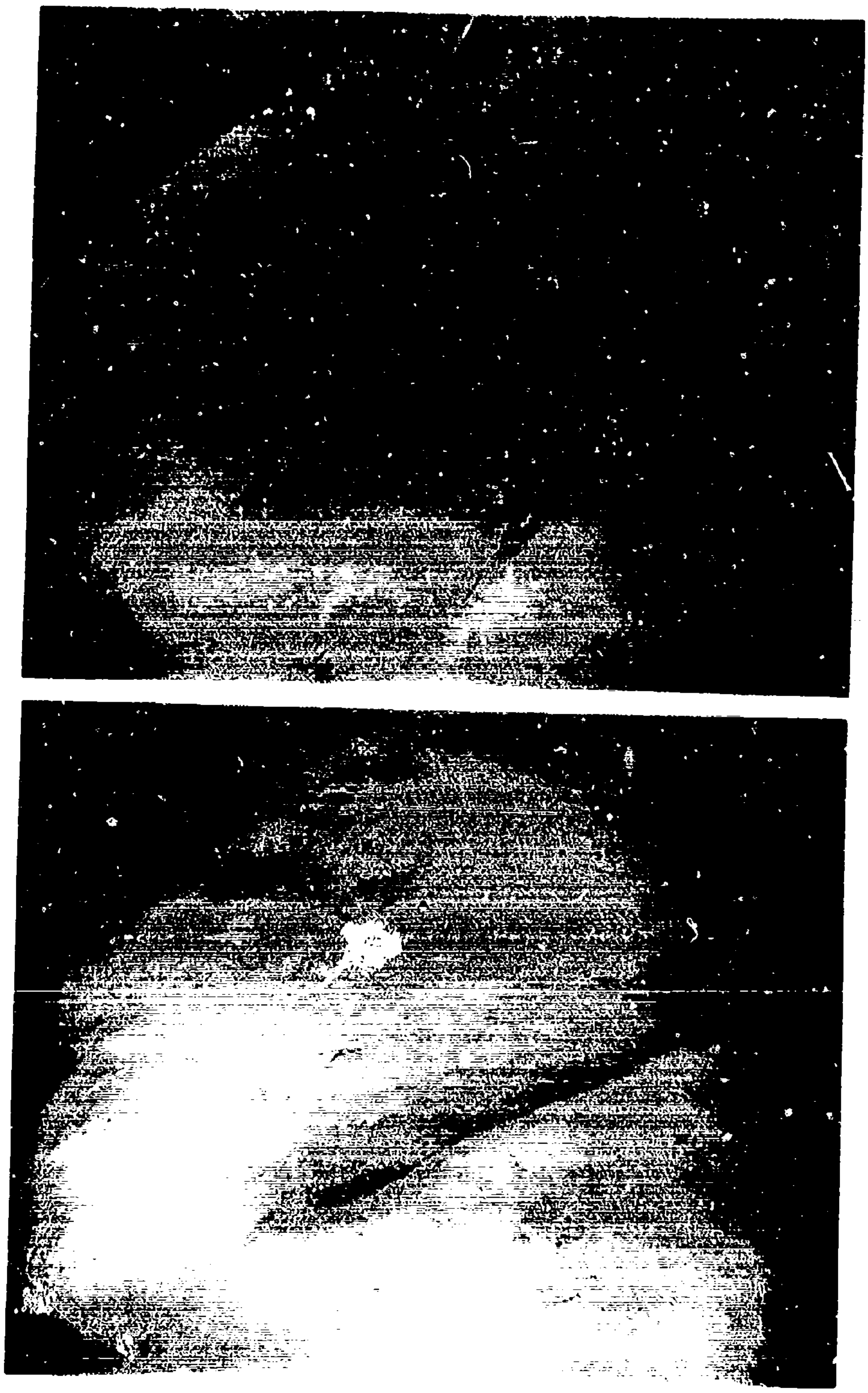

Fig. 10. Bottom photographs showing longitudinal current ripples with approximately 2 m wavelengths.

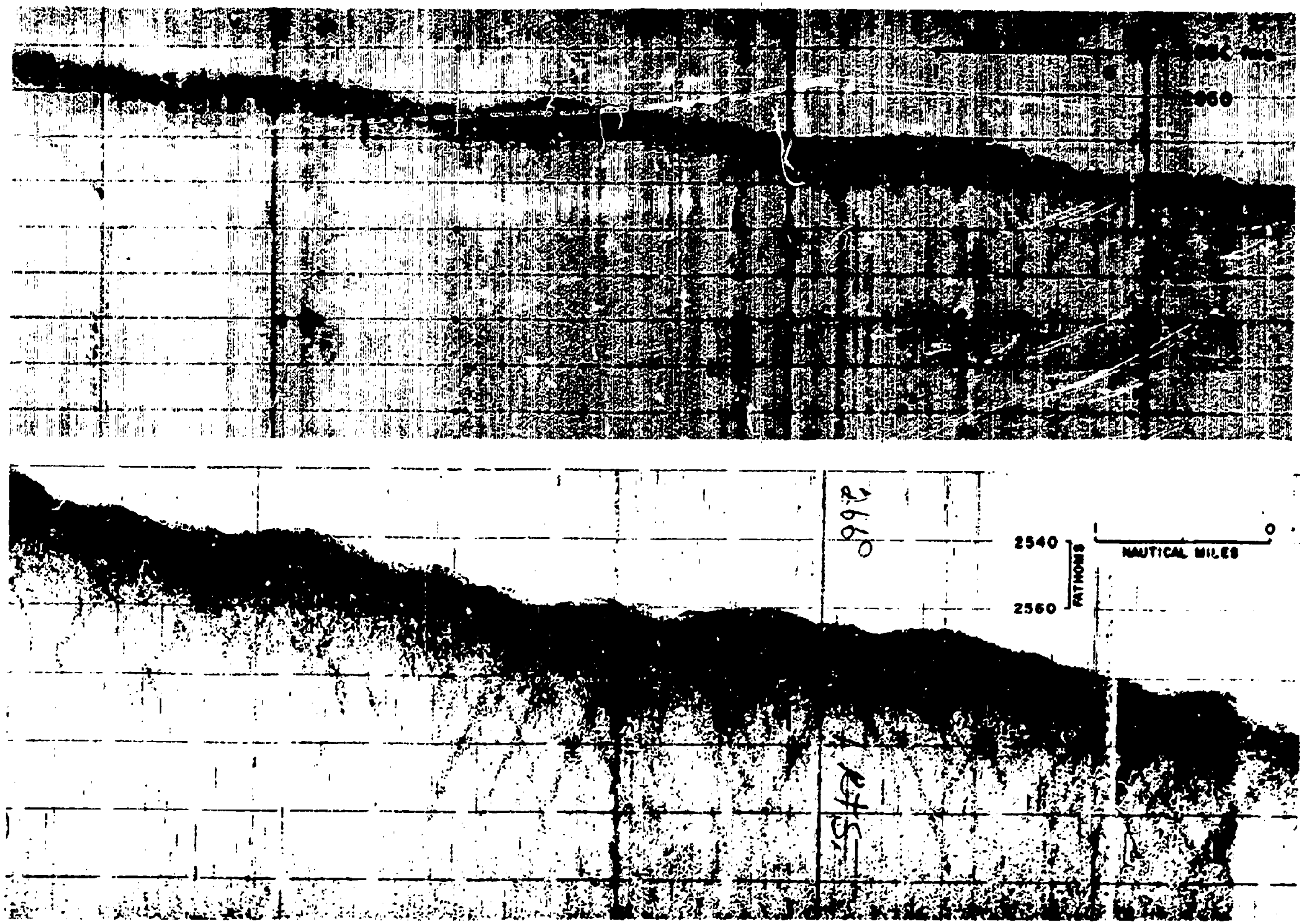

a.

b.

Fig. 11. Incoherent echo sounder traces. (a.) long ping (b.) short ping

Fig. 12. Continuous seismic reflection profiler records from the Blake-Bahama Outer Ridge area.

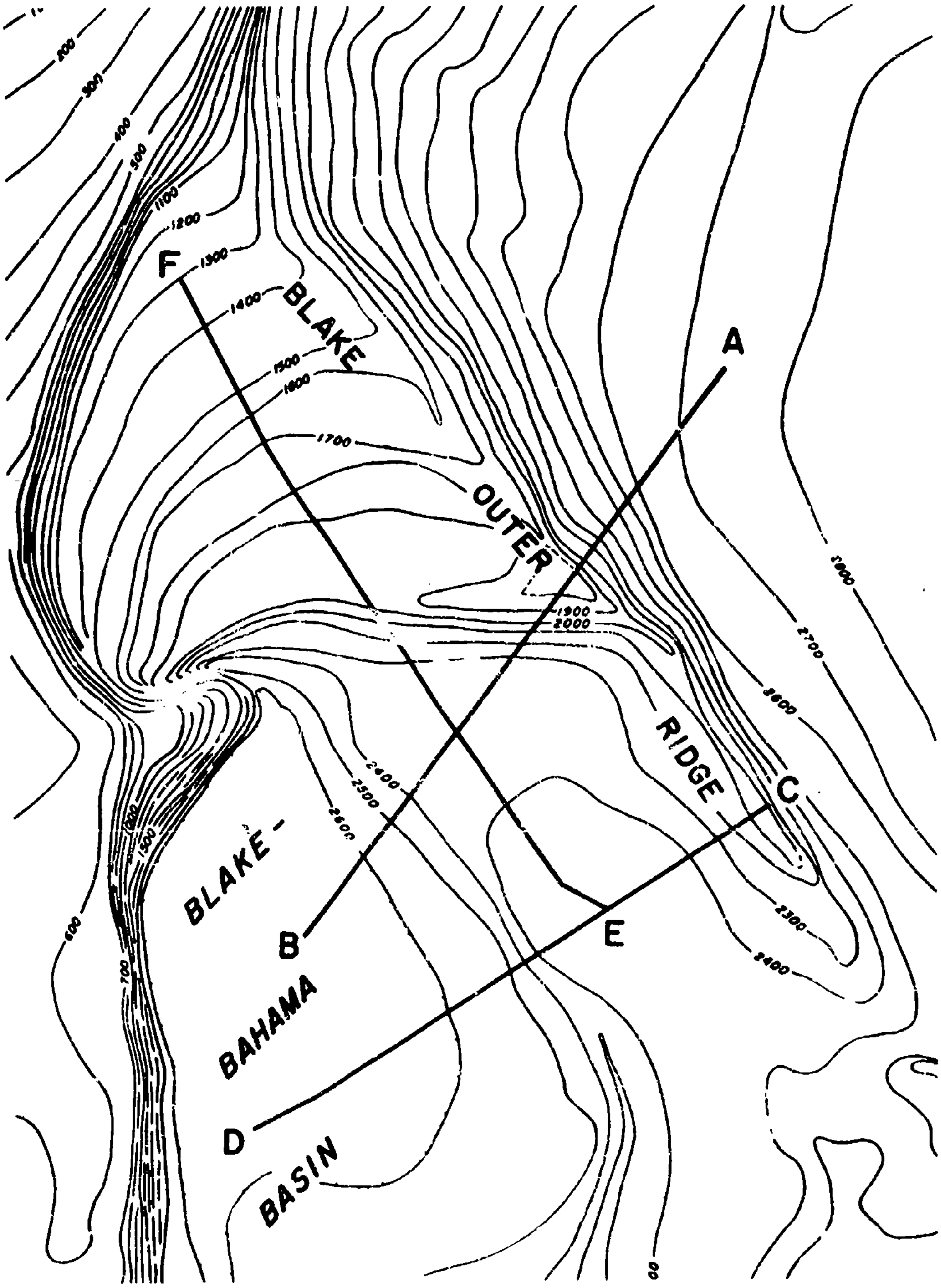

Fig. 13. Location map for Fig. 12.

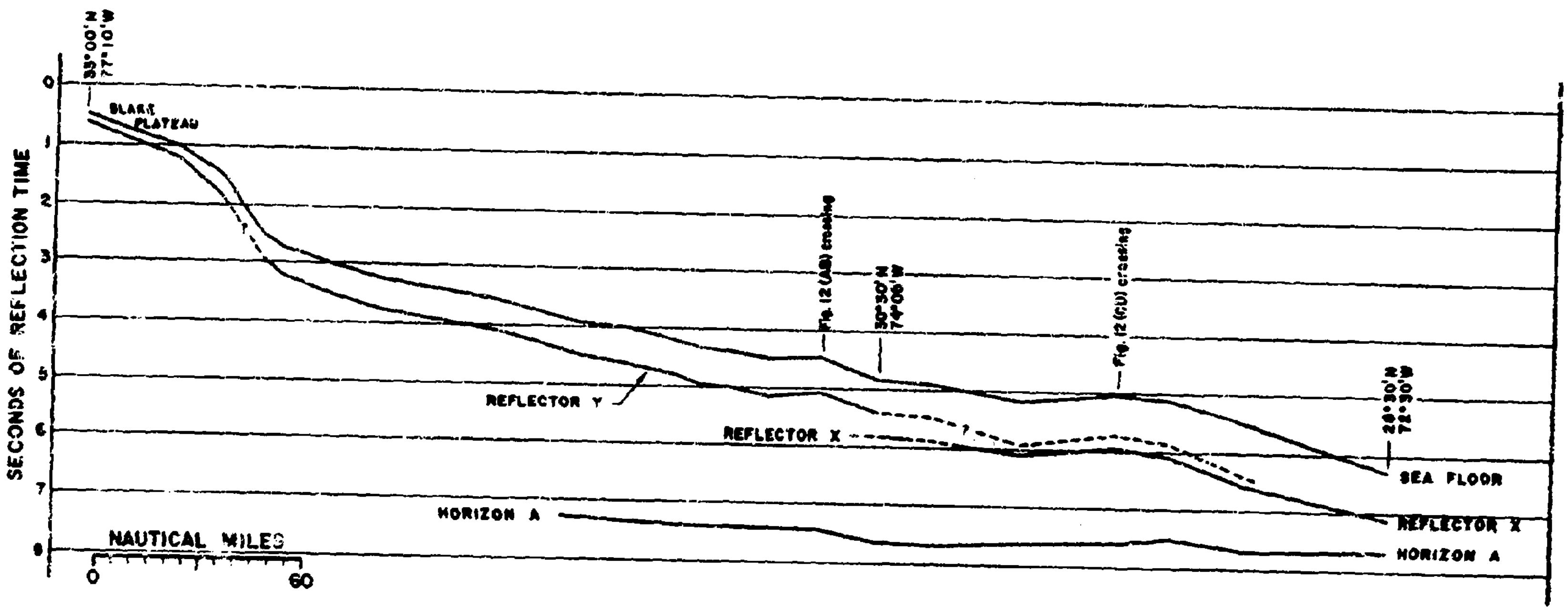

Fig. 14. Structure section along the crest axis of the Blake Outer Ridge.

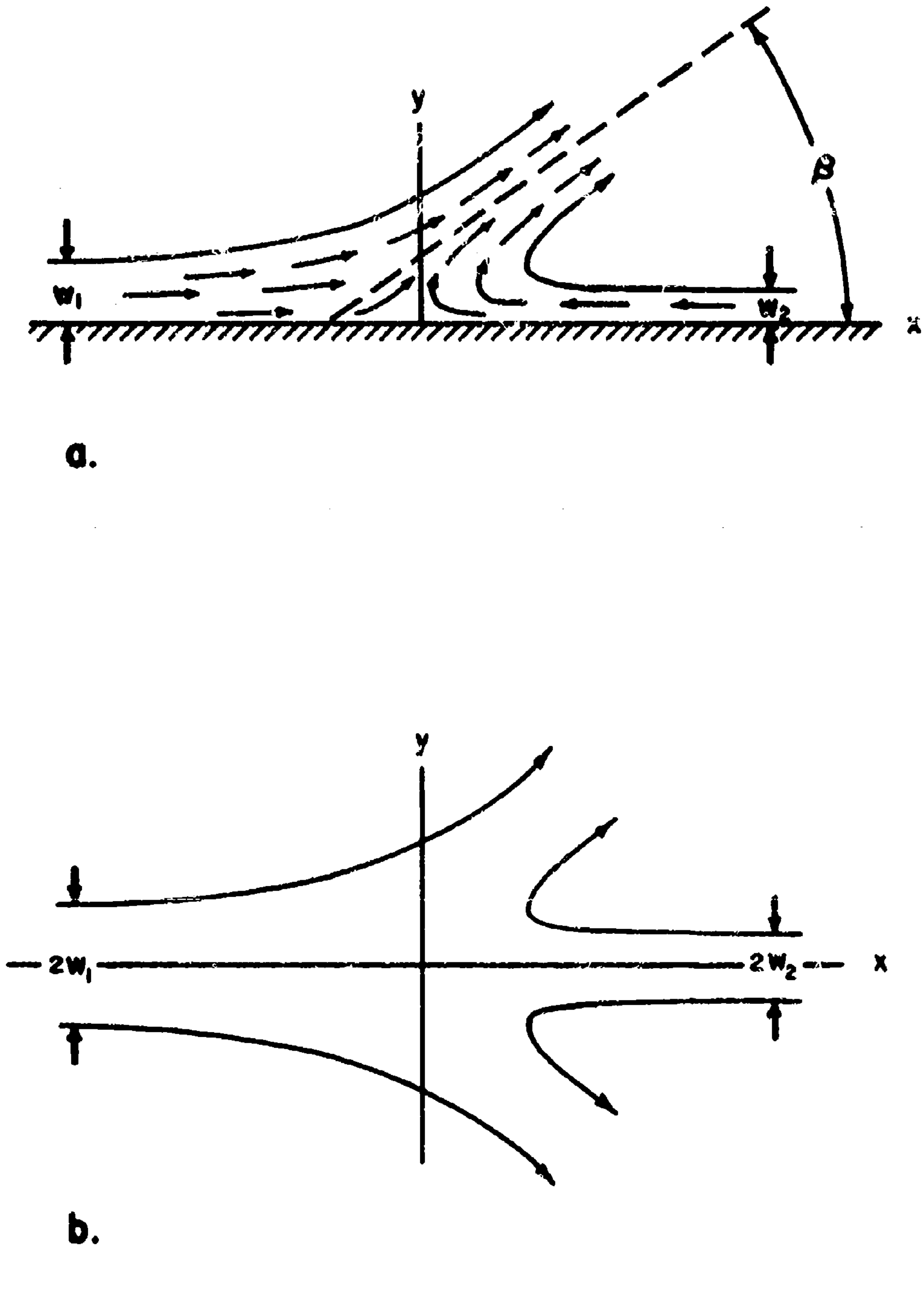

Fig. 15. Flow patterns resulting from impinging currents.
a. rigid boundary along x-axis
b. equivalent pattern for unrestricted currents

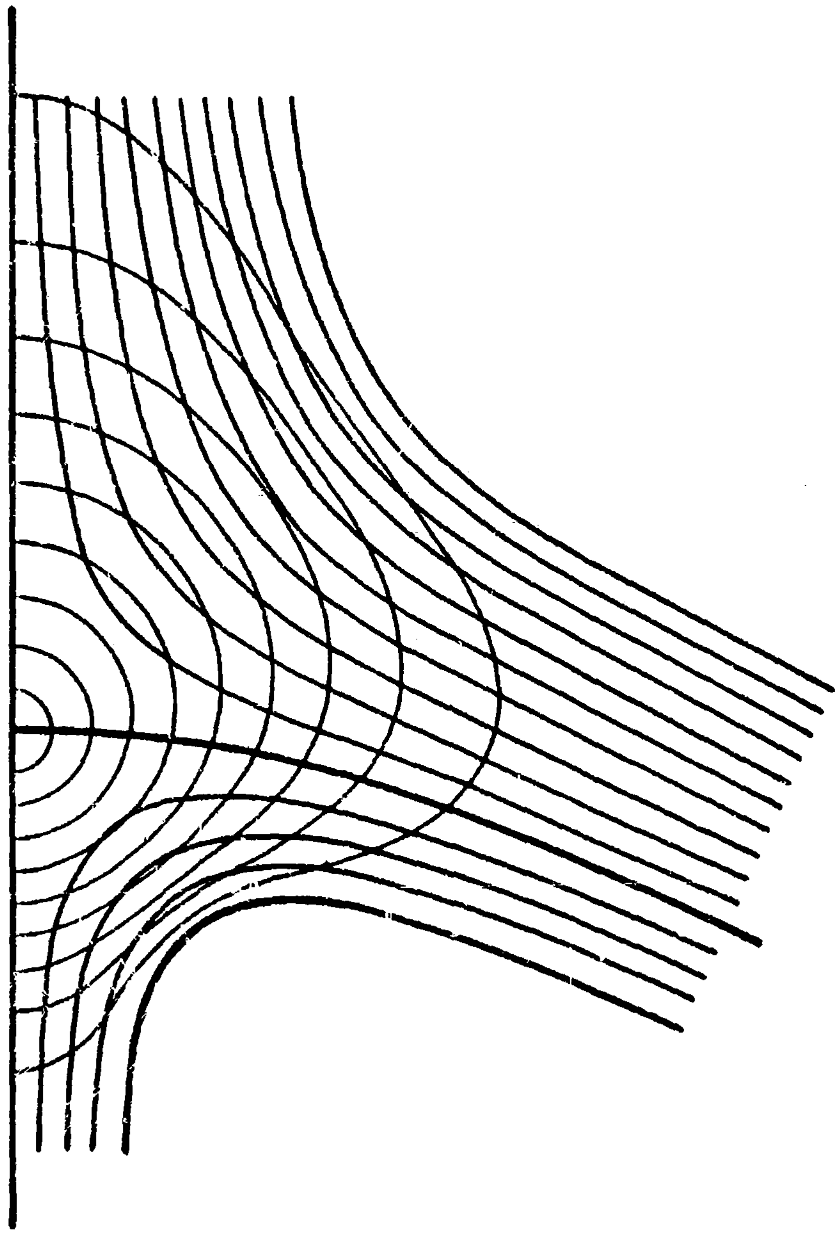

Fig. 16. Streamlines and isotachs computed for $\beta = 66°$. Isotachs are plotted in intervals of 0.1U from zero at the stagnation point to U at the free streamlines.

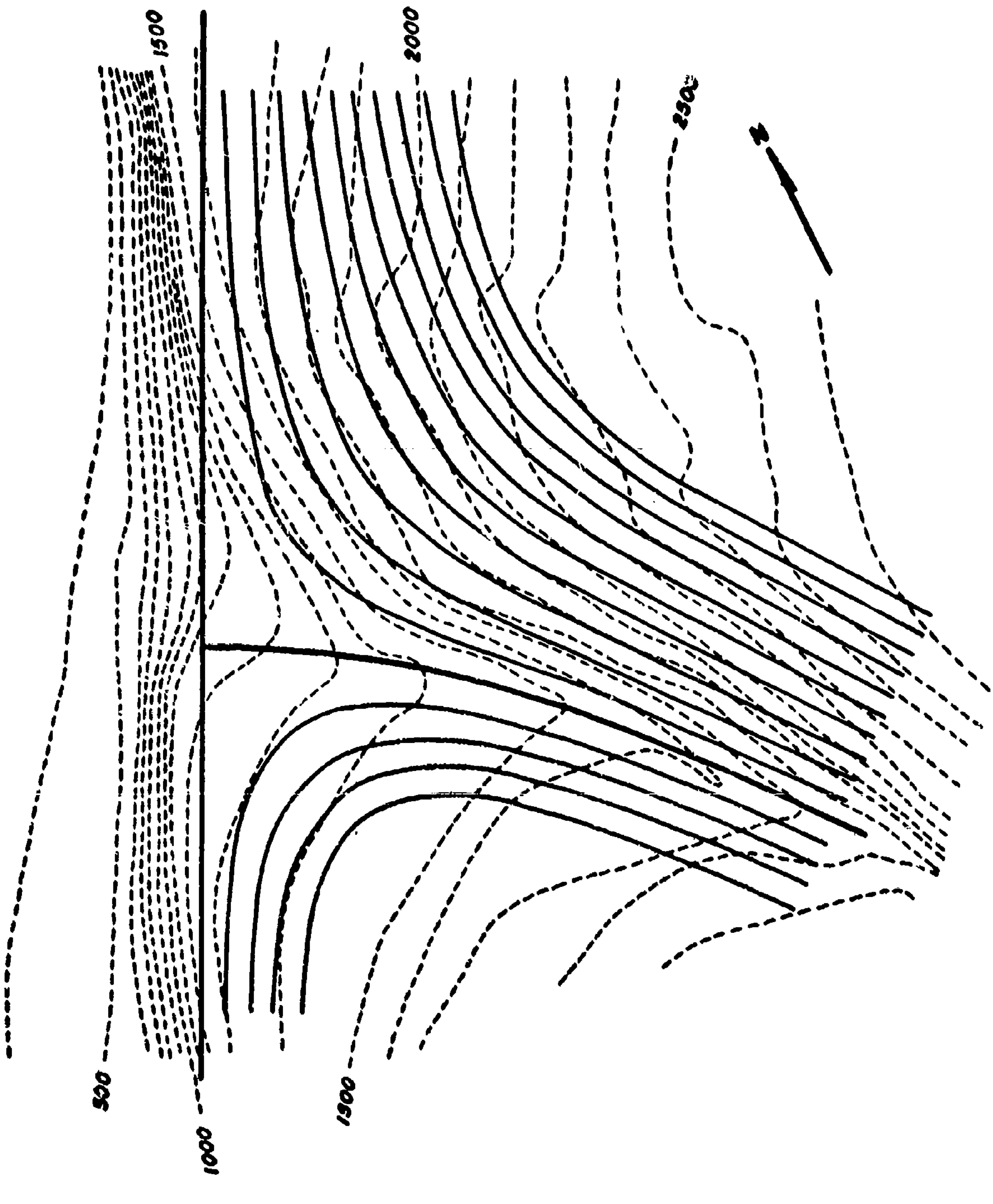

Fig. 17. Comparison of computed streamlines with bathymetric contours.

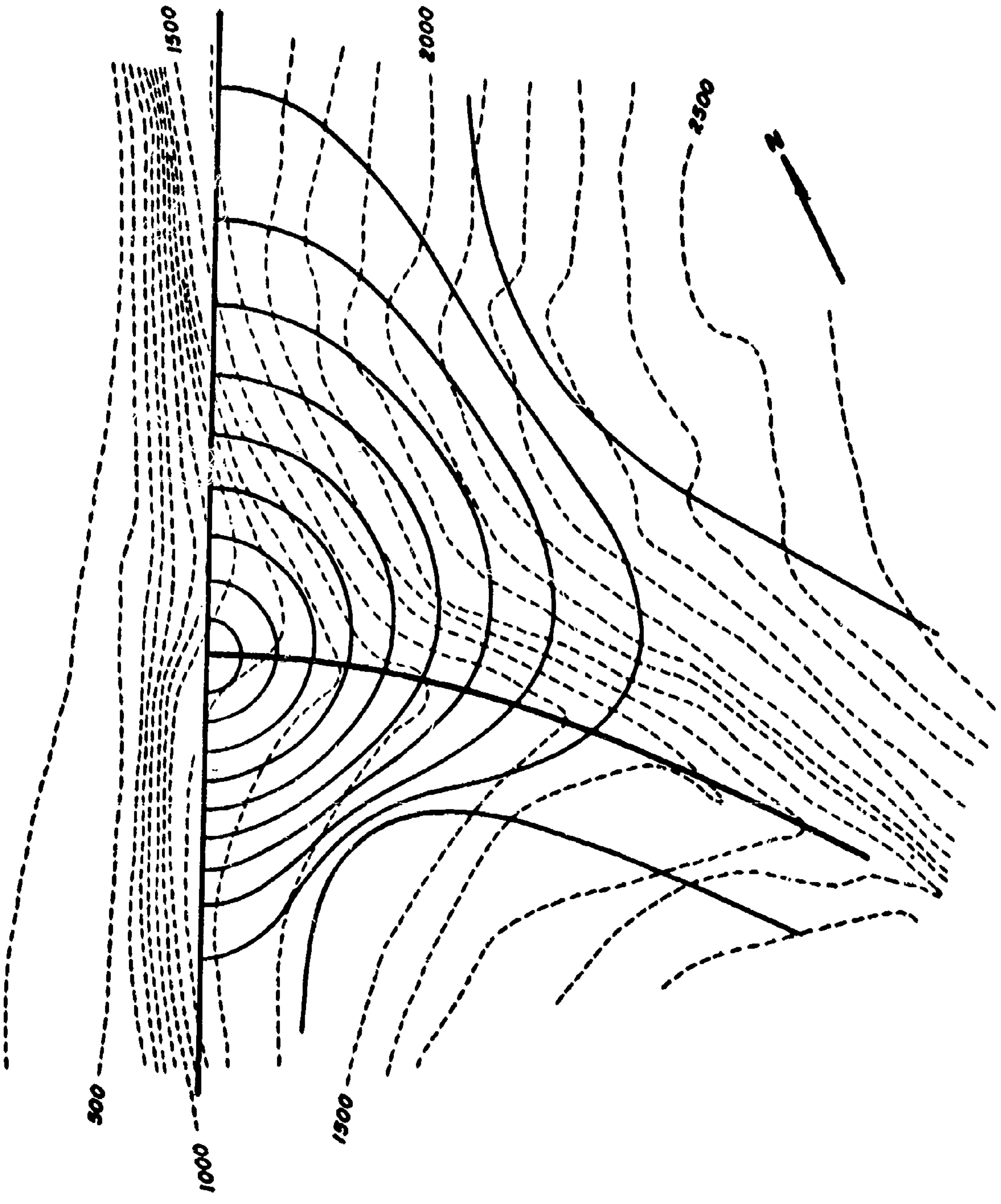

Fig. 18. Comparison of computed isotachs with batl.ymetric contours.

UNCLASSIFIED

Security Classification

DOCUMENT CONTROL DATA - R&D

(Security classification of title, body of abstract and indexing annotation must be entered when the overall report is classified)

1. ORIGINATING ACTIVITY (Corporate author)

Lamont Geological Observatory
Palisades, New York 10964

2a. REPORT SECURITY CLASSIFICATION

unclassified

2b. GROUP

3. REPORT TITLE

Microtopography of the Blake-Bahama Region

4. DESCRIPTIVE NOTES (Type of report and inclusive dates)

Technical Report

5. AUTHOR(S) (Last name, first name, initial)

Bryan, George M. and Markl, Rudi G.

6. REPORT DATE	7a. TOTAL NO. OF PAGES	7b. NO. OF REFS
December 1966	44	17

8a. CONTRACT OR GRANT NO.

NObsr 85077

b. PROJECT AND TASK NO.

c. DOD ELEMENT

d. DOD SUBELEMENT

9a. ORIGINATOR'S REPORT NUMBER(S)

Tech. Report No. 8, CU-8-66

9b. OTHER REPORT NO(S) (Any other numbers that may be assigned this report)

10. AVAILABILITY/LIMITATION NOTICES

Distribution of this document is unlimited.

11. SUPPLEMENTARY NOTES

12. SPONSORING MILITARY ACTIVITY

NAVSHIPS (1622K), Washington, D.C.

13. ABSTRACT

Sea floor microtopography has been shown to have an adverse effect on bottom loss. An attempt has been made through analysis of 12 kc PDR echograms to define (1) the range of wavelengths and (2) the origin, of corrugations observed in the Blake-Bahama Basin and Blake Outer Ridge provinces, as well as to delineate their areal extent.

DD FORM 1 JAN 64 1473

UNCLASSIFIED

Security Classification

UNCLASSIFIED

Security Classification

14. KEY WORDS	LINK A		LINK B		LINK C	
	ROLE	WT	ROLE	WT	ROLE	WT
Effect of Microtopography on Bottom Loss.						
Acoustic propagation						
Blake-Bahama Region						
Bottom Loss						
Marine Geology						
Microtopography						
12 kc echo sounders						

INSTRUCTIONS

1. ORIGINATING ACTIVITY: Enter the name and address of the contractor, subcontractor, grantee, Department of Defense activity or other organization *(corporate author)* issuing the report.

2a. REPORT SECURITY CLASSIFICATION: Enter the overall security classification of the report. Indicate whether "Restricted Data" is included. Marking is to be in accordance with appropriate security regulations.

2b. GROUP: Automatic downgrading is specified in DoD Directive 5200.10 and Armed Forces Industrial Manual. Enter the group number. Also, when applicable, show that optional markings have been used for Group 3 and Group 4 as authorized.

3. REPORT TITLE: Enter the complete report title in all capital letters. Titles in all cases should be unclassified. If a meaningful title cannot be selected without classification, show title classification in all capitals in parenthesis immediately following the title.

4. DESCRIPTIVE NOTES: If appropriate, enter the type of report, e.g., interim, progress, summary, annual, or final. Give the inclusive dates when a specific reporting period is covered.

5. AUTHOR(S): Enter the name(s) of author(s) as shown on or in the report. Enter last name, first name, middle initial. If military, show rank and branch of service. The name of the principal author is an absolute minimum requirement.

6. REPORT DATE: Enter the date of the report as day, month, year, or month, year. If more than one date appears on the report, use date of publication.

7a. TOTAL NUMBER OF PAGES: The total page count should follow normal pagination procedures, i.e., enter the number of pages containing information.

7b. NUMBER OF REFERENCES: Enter the total number of references cited in the report.

8a. CONTRACT OR GRANT NUMBER: If appropriate, enter the applicable number of the contract or grant under which the report was written.

8b, 8c, & 8d. PROJECT NUMBER: Enter the appropriate military department identification, such as project number, subproject number, system numbers, task number, etc.

9a. ORIGINATOR'S REPORT NUMBER(S): Enter the official report number by which the document will be identified and controlled by the originating activity. This number must be unique to this report.

9b. OTHER REPORT NUMBER(S): If the report has been assigned any other report numbers *(either by the originator or by the sponsor)*, also enter this number(s).

10. AVAILABILITY/LIMITATION NOTICES: Enter any limitations on further dissemination of the report, other than those imposed by security classification, using standard statements such as:

(1) "Qualified requesters may obtain copies of this report from DDC."

(2) "Foreign announcement and dissemination of this report by DDC is not authorized."

(3) "U. S. Government agencies may obtain copies of this report directly from DDC. Other qualified DDC users shall request through ________________."

(4) "U. S. military agencies may obtain copies of this report directly from DDC. Other qualified users shall request through ________________."

(5) "All distribution of this report is controlled. Qualified DDC users shall request through ________________."

If the report has been furnished to the Office of Technical Services, Department of Commerce, for sale to the public, indicate this fact and enter the price, if known.

11. SUPPLEMENTARY NOTES: Use for additional explanatory notes.

12. SPONSORING MILITARY ACTIVITY: Enter the name of the departmental project office or laboratory sponsoring *(paying for)* the research and development. Include address.

13. ABSTRACT: Enter an abstract giving a brief and factual summary of the document indicative of the report, even though it may also appear elsewhere in the body of the technical report. If additional space is required, a continuation sheet shall be attached.

It is highly desirable that the abstract of classified reports be unclassified. Each paragraph of the abstract shall end with an indication of the military security classification of the information in the paragraph, represented as *(TS)*, *(S)*, *(C)*, or *(U)*.

There is no limitation on the length of the abstract. However, the suggested length is from 150 to 225 words.

14. KEY WORDS: Key words are technically meaningful terms or short phrases that characterize a report and may be used as index entries for cataloging the report. Key words must be selected so that no security classification is required. Identifiers, such as equipment model designation, trade name, military project code name, geographic location, may be used as key words but will be followed by an indication of technical context. The assignment of links, rules, and weights is optional.

UNCLASSIFIED

Security Classification

END